

# ON THE EXISTENCE OF TRAVELING WAVE SOLUTIONS FOR COLD PLASMAS

DIEGO ALONSO-ORÁN, ANGEL DURÁN, AND RAFAEL GRANERO-BELINCHÓN

ABSTRACT. The present paper is concerned with the existence of traveling wave solutions of the asymptotic model, derived by the authors in a previous work, to approximate the unidirectional evolution of a collision-free plasma in a magnetic field. First, using bifurcation theory, we can rigorously prove the existence of periodic traveling waves of small amplitude. Furthermore, our analysis also evidences the existence of different type of traveling waves. To this end, we present a second approach based on the analysis of the differential system satisfied by the traveling-wave profiles, the existence of equilibria, and the identification of associated homo-clinic and periodic orbits around them. The study makes use of linearization techniques and numerical computations to show the existence of different types of traveling-wave solutions, with monotone and non-monotone behaviour and different regularity, as well as periodic traveling waves.

## CONTENTS

1. Introduction	2
Plan of the paper	3
Acknowledgments	4
2. Notation and auxiliary results	4
3. Existence of periodic traveling wave solutions	5
3.1. Formulation and functional spaces	6
3.2. Spectral and transversality properties of the linearized operator	6
3.3. Proof of Theorem 2	8
4. Traveling wave solutions of the nonlocal wave equation	8
4.1. The case $g \leq g_1(c_s)$	11
4.2. Some previous lemmas	12
5. Existence of non-periodic traveling wave solutions	14
5.1. Dynamics around the equilibrium $y_+$	15
5.2. Dynamics around the equilibrium $y_-$	16
6. Concluding remarks	19
References	21
Appendix A. A procedure for the numerical generation of traveling waves	26

---

*Key words and phrases.* Bifurcation theory, traveling waves, homo-clinic orbits, numerical generation.

## 1. INTRODUCTION

The motion of a magnetized cold plasma consisting of singly-charged particles can be described by the following hyperbolic–hyperbolic–elliptic system of PDEs [8, 17]

$$n_t + (un)_x = 0, \quad (1a)$$

$$u_t + uu_x + \frac{bb_x}{n} = 0, \quad (1b)$$

$$b - n - \left(\frac{b_x}{n}\right)_x = 0, \quad (1c)$$

where  $n$  represents the number density of ions,  $u$  is the ion velocity and  $b$  the magnetic field. In (1) the unknowns are functions of  $(x, t) \in \mathbb{R} \times [0, \infty)$ .

The system (1) was introduced in [17] to study hydromagnetic waves traveling across a magnetic field. Later studies regarding the oblique propagation of hydromagnetic waves were investigated in [8, 23]. The rigorous justification of the KdV limit of (1) is provided in [28]. The first and third author showed in [4] the local well-posedness of classical solutions to (1) with initial data in  $(\rho_0 - 1, u_0) \in H^2(\mathbb{R}) \times H^3(\mathbb{R})$ . Later, in [5], Bae, Choi and Kwon demonstrate that solutions to (1) blow-up in finite time for a certain class of initial data.

Recently in [3], by means a multi-scale expansion approach, the authors derived asymptotic models of (1). The first one is the nonlocal Boussinesq system

$$h_t + (hv)_x + v_x = 0, \quad (2a)$$

$$v_t + vv_x + [\mathcal{L}, \mathcal{N}h]h + \mathcal{N}h = 0, \quad (2b)$$

where the nonlocal operators are given by

$$\mathcal{L} = -\partial_x^2(1 - \partial_x^2)^{-1}, \quad \mathcal{N} = \partial_x(1 - \partial_x^2)^{-1} \text{ (so } \partial_x \mathcal{N} = -\mathcal{L}), \quad (3)$$

with Fourier symbols

$$\widehat{\mathcal{L}h}(\xi) = \frac{\xi^2}{1 + \xi^2} \hat{h}(\xi), \quad \widehat{\mathcal{N}h}(\xi) = \frac{i\xi}{1 + \xi^2} \hat{h}(\xi),$$

and where  $[\mathcal{L}, \cdot] \cdot$  denotes the commutator

$$[\mathcal{L}, f]g = \mathcal{L}(fg) - f\mathcal{L}g.$$

In (2)  $h$  and  $v$  represent, respectively, second-order approximations in a multi-scale expansion of the ionic density and ionic velocity variables. An additional assumption concerning the first-order terms of the expansions leads to the single, unidirectional, nonlocal wave equation for  $h$  given by

$$h_t = -\frac{1}{2}(3hh_x - [\mathcal{L}, \mathcal{N}h]h - \mathcal{N}h - h_x). \quad (4)$$

Furthermore, besides the derivation of (2) and (4), the well-posedness of the corresponding initial-value problems (ivp's) and additional properties, such as the Hamiltonian structure, existence of conserved quantities and the formation of singularities in finite time are also studied in [3].

Our next step in the analysis of (2) and (4) is concerned with the existence of traveling wave solutions. These are solutions of permanent form and traveling with some constant velocity. Their

determination transforms (2) and (4) into the corresponding ordinary differential equations for the wave profiles, depending on the speed. If the profiles are known to go to zero asymptotically (surely along with their derivatives up to some order), that is, if the profiles are localized, they are usually called solitary waves. The present paper is focused on the unidirectional equation (4), while the system (2) will be considered in a forthcoming work.

The study of the existence of solitary wave solutions, specially for models in water wave theory, may be accomplished with several, classical theories, e. g. [6, 20, 26, 27, 30]. In the first result provided in this manuscript we are able to rigorously show the existence of periodic traveling waves of small amplitude and  $O(1)$  velocity, cf. [3]. The proof hinges on non-linear bifurcation techniques via Crandall-Rabinowitz theorem. The bifurcation approach to prove the existence of traveling waves for different equations has been used by different authors [2, 12, 24, 25].

Furthermore, we will also make some formal arguments and simulations that evidence the existence of traveling waves of different type. More precisely, we show a picture on the existence of different types of traveling-wave solutions of (4) (including, but not only, those of solitary type). This approach is based on the following contributions:

- The identification of a reformulation of (4) with only local terms.
- The corresponding differential (ode) systems for the traveling wave profiles are shown to have several remarkable properties which allow to determine and classify different families of equilibria, according to the speed of the wave, used as bifurcation parameter.
- In addition, the reversible character of the ode systems can be used to analyze the dynamics of some of these equilibria from the literature on the emergence and homo-clinic and periodic orbits via linearization and Normal Form theory for reversible vector fields, [9, 18, 20]. Their application reveals the existence of different types of traveling wave solutions, with monotone and non-monotone behaviour and different regularity, as well as smooth solitary waves and periodic traveling waves.
- The discussion is supported by some experiments from an efficient numerical procedure to compute approximations to the profiles. The numerical results suggest some additional properties of the waves, concerning amplitude, speed and decay at infinity.

**Plan of the paper.** The paper is structured as follows. In section 2 we fix the notation and present some auxiliary results on bifurcation theory. In section 3 the existence of smooth periodic traveling waves of small amplitude is proved via a bifurcation argument. Section 4 is devoted to derive the local formulation of (4) and to identify the families of equilibria of the corresponding ode system satisfied by the traveling waves. For two of these equilibria and from the reversibility property of the differential equations, the existence of traveling wave solutions as homo-clinic and periodic orbits around them is discussed in section 5. The discussion is based on the application of normal form theory of the corresponding reversible vector fields, [18], with the help of literature for similar equations, (cf., among others, [9–11, 15, 20] and references therein), and the numerical experiments of generation of approximate waves. Some concluding remarks are outlined in section 6. The numerical procedure to compute approximations of traveling wave profiles is described in appendix A.

**Acknowledgments.** The authors gratefully acknowledge Claudia García for fruitful discussions regarding bifurcation theory and Daniel Sánchez Simón del Pino for pointing out the reference of Lemma 2.1. D.A-O is supported by the fellowship of the Santander-ULL program. D.A-O and R. G-B are also supported by the project “Análisis Matemático Aplicado y Ecuaciones Diferenciales” Grant PID2022- 141187NB-I00 funded by MCIN/ AEI and acronym “AMAED”. This paper is part of the project PID2022-141187NB-I00 with acronym *AMAED* funded by MICIU/AEI /10.13039/501100011033 and by FEDER, UE/AEI /10.13039/501100011033 / FEDER, UE. A.D. is supported by the Spanish Agencia Estatal de Investigación under Research Grant PID2023-147073NB-100.

## 2. NOTATION AND AUXILIARY RESULTS

In this section, we fix the notation used throughout the paper and recall some classical results on bifurcation theory. For a periodic function  $f$  with values in  $\mathbb{R}$  we define the Hölder norms as

$$\begin{aligned} \|f\|_{C^0(\mathbb{T})} &= \sup_{x \in \mathbb{T}^1} |f|, \quad \|f\|_{C^k(\mathbb{T})} = \|f\|_{C^0(\mathbb{T})} + \sum_{\ell=1}^k \left\| \partial_x^\ell f \right\|_{C^0(\mathbb{T})}, \quad k \in \mathbb{N}, \\ \|f\|_{C^{0,\alpha}(\mathbb{T})} &= \|f\|_{C^0(\mathbb{T})} + \sup_{x_1, x_2 \in \mathbb{T}} \frac{|f(x_1) - f(x_2)|}{|x_1 - x_2|^\alpha}, \quad 0 < \alpha < 1, \\ \|f\|_{C^{k,\alpha}(\mathbb{T})} &= \|f\|_{C^{k-1}(\mathbb{T})} + \left\| \partial_x^k f \right\|_{C^\alpha(\mathbb{T})}, \quad k \in \mathbb{N}, \quad 0 < \alpha < 1. \end{aligned}$$

The Banach space of continuous functions for which the above norms are finite will be denoted  $C^k(\mathbb{T})$  and  $C^{k,\alpha}(\mathbb{T})$ .

We denote by  $\mathcal{Q} := (I - \partial_{xx}^2)^{-1}$  the Helmholtz operator with Fourier symbol

$$\widehat{\mathcal{Q}f}(\xi) = \frac{1}{1 + \xi^2} \widehat{f}(\xi).$$

Acting on square integrable periodic functions  $f$ , the Helmholtz operator has the representation

$$\mathcal{Q}f(x) = [(I - \partial_{xx}^2)^{-1}]f(x) = [\mathbf{G}_{\mathbb{T}} \star f](x), \quad (5)$$

where the Green function  $\mathbf{G}_{\mathbb{T}}$  is explicitly given by

$$\mathbf{G}_{\mathbb{T}}(x) = \frac{\cosh(x - 2\pi[\frac{x}{2\pi}] - \pi)}{2 \sinh(\pi)}. \quad (6)$$

We have the following bound whose proof can be found in [29, Theorem 4, §4.4]:

**Lemma 2.1.** *The operator  $\mathcal{Q}$  maps  $C^{k,\alpha}(\mathbb{T})$  isomorphically onto  $C^{k+2,\alpha}(\mathbb{T})$ . More precisely, there exists a constant  $C > 0$  such that*

$$\|\mathcal{Q}f\|_{C^{k+2,\alpha}(\mathbb{T})} \leq C \|f\|_{C^{k,\alpha}(\mathbb{T})}, \quad f \in C^{k,\alpha}(\mathbb{T}), \quad k \in \mathbb{N} \cup \{0\}. \quad (7)$$

Therefore as a direct consequence the non-local operators in (3) written as

$$\mathcal{L} = -\partial_x^2 \mathcal{Q}, \quad \mathcal{N} = \partial_x \mathcal{Q}. \quad (8)$$

enjoyed the following estimates

$$\|\mathcal{L}f\|_{C^{k,\alpha}(\mathbb{T})} \leq C \|f\|_{C^{k,\alpha}(\mathbb{T})}, \quad \|\mathcal{N}f\|_{C^{k+1,\alpha}(\mathbb{T})} \leq C \|f\|_{C^{k,\alpha}(\mathbb{T})}. \quad (9)$$

The previous bounds (7)-(9) are particular cases of a more general theory of mapping properties for pseudo-differential operators in Besov spaces, cf. [1, Theorem 6.19, §6.6].

Next, let us revisit the Crandall-Rabinowitz Theorem, an essential tool in bifurcation theory that we will use to show the existence of smooth periodic traveling waves. Before we dive in, let us first go over the following definition:

**Definition 1** (Fredholm operator). Let  $X$  and  $Y$  be two Banach spaces. A continuous linear mapping  $T : X \rightarrow Y$ , is a Fredholm operator if it fulfills the following properties,

- (1)  $\dim \text{Ker } T < \infty$ ,
- (2)  $\text{Im } T$  is closed in  $Y$ ,
- (3)  $\text{codim Im } T < \infty$ .

The integer  $\dim \text{Ker } T - \text{codim Im } T$  is called the Fredholm index of  $T$ . Moreover, we also remark that the index of a Fredholm operator remains unchanged under compact perturbations, cf. [21, 22]. Next, let us state the classical Crandall-Rabinowitz theorem [13] which reads as follows:

**Theorem 1** (Crandall-Rabinowitz Theorem). *Let  $X, Y$  be two Banach spaces,  $V$  be a neighborhood of 0 in  $X$  and  $F : \mathbb{R} \times V \rightarrow Y$  be a function with the properties,*

- (1)  $F(\lambda, 0) = 0$  for all  $\lambda \in \mathbb{R}$ .
- (2) *The partial derivatives  $\partial_\lambda F$ ,  $\partial_f F$  and  $\partial_\lambda \partial_f F$  exist and are continuous.*
- (3) *The operator  $\partial_f F(\lambda_0, 0)$  is Fredholm of zero index and  $\text{Ker}(\partial_f F(\lambda_0, 0)) = \langle f_0 \rangle$  is one-dimensional.*
- (4) *Transversality assumption:  $\partial_\lambda \partial_f F(\lambda_0, 0) f_0 \notin \text{Im}(\partial_f F(\lambda_0, 0))$ .*

*If  $Z$  is any complement of  $\text{Ker}(\partial_f F(\lambda_0, 0))$  in  $X$ , then there is a neighborhood  $U$  of  $(\lambda_0, 0)$  in  $\mathbb{R} \times X$ , an interval  $(-a, a)$ , and two continuous functions  $\Phi : (-a, a) \rightarrow \mathbb{R}$ ,  $\beta : (-a, a) \rightarrow Z$  such that  $\Phi(0) = \lambda_0$  and  $\beta(0) = 0$  and*

$$F^{-1}(0) \cap U = \{(\Phi(s), s f_0 + s \beta(s)) : |s| < a\} \cup \{(\lambda, 0) : (\lambda, 0) \in U\}.$$

In this context, we will say that  $\lambda_0$  is an eigenvalue of  $F$ .

### 3. EXISTENCE OF PERIODIC TRAVELING WAVE SOLUTIONS

This section is devoted to show the existence of smooth periodic traveling waves of small amplitude. The precise statement of result reads:

**Theorem 2.** *For any  $m \geq 1$  there exists a one dimensional curve  $s \mapsto (c_s, \varphi_s)$ , with  $s \in I$ , such that*

$$h(x) = \varphi_s(x) \in C^{1,\alpha}([0, 2\pi], \mathbb{R}),$$

*is a  $m$ -fold traveling wave solution to (4) with constant speed  $c_s$ .*

**3.1. Formulation and functional spaces.** We look for periodic traveling waves for  $h$  and hence we make the Ansatz

$$h(x, t) = \varphi(x - ct),$$

for some speed  $c \in \mathbb{R}$ . Hence, plugging it into (4) we find the problem

$$-c\varphi' = -\frac{1}{2} (3\varphi\varphi' - [\mathcal{L}, \mathcal{N}\varphi]\varphi - \mathcal{N}\varphi - \varphi'). \quad (10)$$

As a consequence, the equation reduces to

$$F[c, \varphi](\xi) = 0, \quad \xi \in [-\pi, \pi],$$

where

$$F[c, \varphi](\xi) = \frac{1}{2} (3\varphi(\xi)\varphi'(\xi) - [\mathcal{L}, \mathcal{N}\varphi(\xi)]\varphi(\xi) - \mathcal{N}\varphi(\xi) - \varphi'(\xi)) - c\varphi'(\xi). \quad (11)$$

We observe that, regardless of the value of  $c$  we have the following line of trivial solutions

$$F[c, 0] = 0.$$

Following [2], we define the functional spaces

$$X := \left\{ h \in C^{1,\alpha}([0, 2\pi], \mathbb{R}), \quad h(\xi) = \sum_{k \geq 1} h_k \cos(k\xi) \text{ with norm } \|h\|_X = \|h\|_{C^{1,\alpha}} \right\},$$

$$Y := \left\{ h \in C^{0,\alpha}([0, 2\pi], \mathbb{R}), \quad h(\xi) = \sum_{k \geq 1} h_k \sin(k\xi) \text{ with norm } \|h\|_Y = \|h\|_{C^{0,\alpha}} \right\}.$$

Furthermore, we also introduce the space

$$Z := \left\{ h \in C^{2,\alpha}([0, 2\pi], \mathbb{R}), \quad h(\xi) = \sum_{k \geq 1} h_k \sin(k\xi) \text{ with norm } \|h\|_Z = \|f\|_{C^{2,\alpha}} \right\}.$$

It is straightforward to check that the embedding  $Z \hookrightarrow Y$  is compact.

**3.2. Spectral and transversality properties of the linearized operator.** In this subsection, we will check that the hypothesis of the Crandall-Rabinowitz Theorem 1 are satisfied. To start with, let us show that the operator  $F : \mathbb{R} \times X \rightarrow Y$  given in (11) is well-defined and  $\mathcal{C}^1(\mathbb{R} \times X \rightarrow Y)$ . We first observe that if  $\varphi$  is an even function,  $\varphi(\xi) = \varphi(-\xi)$ , then  $F[c, \varphi]$  is an odd function, i.e.,

$$F[c, \varphi](\xi) = -F[c, \varphi](-\xi).$$

To that purpose, we first notice that  $\varphi'(-\xi) = -\varphi'(\xi)$ . Moreover, using the representation (5)-(6) for the Helmholtz operator, we easily check that

$$\mathcal{Q}\varphi(\xi) = \mathcal{Q}\varphi(-\xi).$$

Invoking (8) we find that

$$\mathcal{N}\varphi(\xi) = \mathcal{Q}\varphi'(\xi) = -\mathcal{N}\varphi(-\xi), \quad \mathcal{L}\varphi(\xi) = (I - \mathcal{Q})\varphi(\xi) = \mathcal{L}\varphi(-\xi),$$

and hence  $[\mathcal{L}, \mathcal{N}\varphi]\varphi(\xi) = -[\mathcal{L}, \mathcal{N}\varphi]\varphi(-\xi)$ . Thus, by combining the previous identities and recalling (11) we conclude that  $F[c, \varphi](\xi) = -F[c, \varphi](-\xi)$  satisfying the symmetry property.

In the following let us show that  $F : \mathbb{R} \times X \rightarrow Y$  is well-defined. It is straightforward to check that

$$\left\| -\frac{1}{2} (\mathcal{N}\varphi + \varphi') - c\varphi' \right\|_Y \leq C \|\varphi\|_X.$$

Similarly, the non-linear terms can be bounded by

$$\left\| \frac{1}{2} (3\varphi\varphi' - [\mathcal{L}, \mathcal{N}\varphi]\varphi) \right\|_Y \leq C \|\varphi\|_X \|\varphi\|_Y + \|\varphi\|_Y^2,$$

where we have used estimate (9) and the fact that

$$\|fg\|_Y \leq \|f\|_Y \|g\|_Y.$$

Thus, since  $X \hookrightarrow Y$ , we conclude that

$$\|F[c, \varphi]\|_Y \leq C (\|\varphi\|_X^2 + \|\varphi\|_X).$$

In order to prove that  $F \in \mathcal{C}^1(\mathbb{R} \times X \rightarrow Y)$  it is sufficient to show that the Gateaux derivative of  $F$  verifies

$$\|\partial_\varphi F[c, \varphi_1]f - \partial_\varphi F[c, \varphi_2]f\|_Y \leq C \|f\|_X \|\varphi_1 - \varphi_2\|_X. \quad (12)$$

We compute the Gateaux derivative of  $F$  and find that

$$\partial_\varphi F[c, \varphi]f = \frac{3}{2}\varphi'f + \frac{3}{2}\varphi f' - [\mathcal{Q}, \mathcal{N}f]\varphi - [\mathcal{Q}, \mathcal{N}\varphi]f - \frac{1}{2}\mathcal{N}f - \frac{1}{2}f' - cf'.$$

Repeating the same estimates by making use of estimates (9) and Lemma 2.1 to deal with the Helmholtz operator  $\mathcal{Q}$  we can easily check that (12) is indeed satisfied. Hence, we can conclude that the Gateaux derivative is continuous (indeed, it is Lipschitz) and then we can ensure the existence and continuity of the Fréchet derivative.

Next, we analyze the linearized operator at the trivial solution which is given by

$$\partial_\varphi F[c, 0]f(\xi) = -\frac{1}{2}\mathcal{N}f(\xi) - \frac{1}{2}f'(\xi) - cf'(\xi) := \mathbf{L}(f)(\xi) + \mathbf{K}(f)(\xi),$$

where

$$\mathbf{L}(f)(\xi) = -\frac{1}{2}f' - cf, \quad \text{and} \quad \mathbf{K}(f)(\xi) = -\frac{1}{2}\mathcal{N}f.$$

The principal part of the operator  $\mathbf{L}f : X \rightarrow Y$  is an isomorphism and hence has zero index. Moreover, using estimate (9), we infer that the operator  $\mathbf{K}f : X \rightarrow Z$  is continuous and the embedding  $Z \hookrightarrow Y$  is compact. Therefore, since the index of a Fredholm operator remains unchanged due to compact perturbations we conclude that  $\partial_\varphi F[c, 0]f$  is a Fredholm operator of zero index.

To conclude we characterize the kernel of the linear operator. For  $f \in X$  we find that

$$\partial_\varphi F[c, 0]f = \sum_{k=1}^{\infty} f_k \sin(kx) \left( -\frac{k}{2(1+k^2)} - \frac{k}{2} - ck \right).$$

Thus, for

$$c_k = -\frac{1}{2(1+k^2)} - \frac{1}{2}$$

we have that

$$\text{Ker}(\partial_\varphi F[c, 0]) = \text{span}(\cos(kx))$$

and, recalling that the linearized operator is Fredholm operator of zero index,

$$Y/\text{Img}(\partial_\varphi F[c, 0]) = \text{span}(\sin(kx)).$$

The transversality condition is then satisfied because

$$\partial_c \partial_\varphi F[c_k, 0]f = \sum_{k=1}^{\infty} f_k \sin(kx) (-k),$$

and, if  $f \in \text{Ker}(\partial_\varphi F[c, 0])$ , then

$$\partial_c \partial_\varphi F[c_k, 0]h = -k f_k \sin(kx) \notin \text{Img}(\partial_\varphi F[c, 0]).$$

**3.3. Proof of Theorem 2.** We have checked that the Crandall-Rabinowitz theorem can be applied in our equation (10). Fix  $m \geq 1$ . In order to prove Theorem 2, let us introduce the symmetry  $m$  in the spaces. For that, let us define

$$X_m := \left\{ f \in C^{1,\alpha}([0, 2\pi]), \quad f(\xi) = \sum_{k \geq 1} f_k \cos(mk\xi) \text{ with norm } \|f\|_{X_m} = \|f\|_{C^{1,\alpha}} \right\},$$

$$Y_m := \left\{ f \in C^{0,\alpha}([0, 2\pi]), \quad f(\xi) = \sum_{k \geq 1} f_k \sin(mk\xi) \text{ with norm } \|f\|_{Y_m} = \|f\|_{C^{0,\alpha}} \right\},$$

for any  $m \geq 1$ . The fact that the operator  $F : \mathbb{R} \times X_m \rightarrow Y_m$  is well-defined and  $\mathcal{C}^1(\mathbb{R} \times X_m \rightarrow Y_m)$  can be checked by repeating the computations of Subsection 3.2. However, we have to show that the  $m$ -fold symmetry property holds. More precisely, we have to prove that if  $\varphi(\xi + \frac{2\pi}{m}) = \varphi(\xi)$  then

$$F[c, \varphi](\xi + \frac{2\pi}{m}) = F[c, \varphi](\xi).$$

Note that if  $\varphi$  has  $m$ -fold symmetry, then all the derivatives of  $\varphi$  also enjoy the same symmetry property. Moreover, recalling that  $\mathcal{Q}$  is a convolution operator (5), the symmetry is also satisfied and thus  $F[c, \varphi](\xi + \frac{2\pi}{m}) = F[c, \varphi](\xi)$  follows. The rest of the arguments can be argued similarly as in the previous Subsection 3.2. Thus, Crandall-Rabinowitz theorem can be applied obtaining Theorem 2.

#### 4. TRAVELING WAVE SOLUTIONS OF THE NONLOCAL WAVE EQUATION

In this section the existence of traveling wave solutions of the unidirectional model is analyzed. Note first, [3], that (4) can be written in the alternative form

$$h_t + \partial_x \left( \frac{3}{4}h^2 + \frac{1}{2}\mathcal{N}(h\mathcal{N}h) - \frac{1}{4}(\mathcal{N}h)^2 - \frac{1}{2}\mathcal{Q}h - \frac{h}{2} \right) = 0. \quad (13)$$

An additional property that will be used below is a formulation of (4) involving local terms: if

$$\mathcal{J} = \mathcal{Q}^{-1}, h = \mathcal{J}u, \quad (14)$$

then (13) can be written as

$$\mathcal{J}u_t + \partial_x \left( \frac{3}{4}(\mathcal{J}u)^2 + \frac{1}{2}\partial_x \mathcal{J}^{-1}((\mathcal{J}u)\partial_x u) - \frac{1}{4}(\partial_x u)^2 - \frac{1}{2}u - \frac{\mathcal{J}u}{2} \right) = 0. \quad (15)$$



For traveling wave solutions  $h = h(x - c_s t)$  of (13), the profiles  $h = h(X)$ ,  $X = x - c_s t$  must satisfy

$$-c_s h + \left( \frac{3}{4} h^2 + \frac{1}{2} \mathcal{N}(h \mathcal{N} h) - \frac{1}{4} (\mathcal{N} h)^2 - \frac{1}{2} \mathcal{Q} h - \frac{h}{2} \right) + g = 0, \quad (16)$$

with  $g$  constant. In terms of the variable  $u$ , defined in (14), (16) yields

$$-c_s \mathcal{J}^2 u + \left( \frac{3}{4} \mathcal{J} (\mathcal{J} u)^2 + \frac{1}{2} \partial_x ((\mathcal{J} u) \partial_x u) - \frac{1}{4} \mathcal{J} (\partial_x u)^2 - \frac{1}{2} \mathcal{J} u - \frac{\mathcal{J}^2 u}{2} \right) = 0, \quad (17)$$

which can be written as

$$\begin{aligned} & \left( \frac{3}{2} \mathcal{J} u - \tilde{c}_s \right) u'''' - \left( 2\tilde{c}_s + \frac{1}{2} \right) u'' + \left( \tilde{c}_s + \frac{1}{2} \right) u \\ & \quad = \tilde{f}(u, u', u'', u''') = f(u, u', u'', u''') + g \\ & = \frac{1}{2} \left( \frac{3}{2} u^2 + \frac{7}{2} (u')^2 + uu'' - \frac{3}{2} (u'')^2 - 6u'u''' + 3(u''')^2 \right) + g, \end{aligned} \quad (18)$$

where  $\tilde{c}_s = c_s + \frac{1}{2}$ . Equation (17) can also be formulated as a first-order system for  $Y = (y_1, y_2, y_3, y_4)^T = (u, u', u'', u''')^T$  as

$$\begin{aligned} \frac{dy_1}{dX} &= y_2, \\ \frac{dy_2}{dX} &= y_3, \\ \frac{dy_3}{dX} &= y_4, \\ \frac{dy_4}{dX} &= \frac{1}{\alpha(y_1, y_3, \tilde{c}_s)} (g + F(Y)), \end{aligned} \quad (19)$$

where

$$\alpha(y_1, y_3, \tilde{c}_s) = \frac{3}{2}(y_1 - y_3) - \tilde{c}_s, \quad (20)$$

$$\begin{aligned} F(Y) &= \left( 2\tilde{c}_s + \frac{1}{2} \right) y_3 - \left( \tilde{c}_s + \frac{1}{2} \right) y_1 \\ & \quad + \frac{1}{2} \left( \frac{3}{2} y_1^2 + \frac{7}{2} y_2^2 + y_1 y_3 - \frac{3}{2} y_3^2 - 6y_2 y_4 + 3y_4^2 \right). \end{aligned} \quad (21)$$

The system (19)-(21) has a singularity as  $\alpha = 0$ , meaning that

$$\frac{3}{2} \mathcal{J} u - \tilde{c}_s = 0 \Rightarrow h = \frac{2}{3} \tilde{c}_s.$$

Out of this constant solution, the transformation  $dX = \alpha dZ$  leads to the nonsingular system, [31]

$$\begin{aligned} \frac{dy_1}{dZ} &= \alpha y_2, \\ \frac{dy_2}{dZ} &= \alpha y_3, \\ \frac{dy_3}{dZ} &= \alpha y_4, \\ \frac{dy_4}{dZ} &= g + F(Y), \end{aligned} \quad (22)$$

We first discuss the equilibria of (22). There are two cases:

(i)  $\alpha = 0$ . Then

$$y_1 = y_3 + \frac{2}{3} \left( c_s + \frac{1}{2} \right).$$

Furthermore, after some tedious algebra, the condition  $g + F(Y) = 0$  can be written as

$$\frac{7}{2}x_1^2 + \frac{3}{7}x_2^2 + x_3^2 + 2(g - g_2(c_s)) = 0, \quad (23)$$

where

$$x_1 = y_2 - \frac{6}{7}y_4, \quad x_2 = y_4, \quad x_3 = y_3 + \frac{7}{3} \left( c_s + \frac{1}{2} \right), \quad (24)$$

and

$$g_2(c_s) := \frac{1}{3} \left( c_s + \frac{1}{2} \right) + \frac{52}{9} \left( c_s + \frac{1}{2} \right). \quad (25)$$

Note that:

- If  $g > g_2(c_s)$ , there are no points  $(x_1, x_2, x_3)$  satisfying (23).
- If  $g = g_2(c_s)$ , the only point satisfying (23) is  $x_1 = x_2 = x_3 = 0$ . Since the inverse of (24) is

$$y_2 = x_1 + \frac{6}{7}x_2, \quad y_4 = x_2, \quad y_3 = x_3 - \frac{7}{3} \left( c_s + \frac{1}{2} \right), \quad (26)$$

and

$$y_1 = y_3 + \frac{2}{3} \left( c_s + \frac{1}{2} \right) = x_3 - \frac{5}{3} \left( c_s + \frac{1}{2} \right), \quad (27)$$

then the origin is transformed into

$$y_1 = -\frac{5}{3} \left( c_s + \frac{1}{2} \right), \quad y_2 = 0, \quad y_3 = -\frac{7}{3} \left( c_s + \frac{1}{2} \right), \quad y_4 = 0.$$

- If  $g < g_2(c_s)$ , then we have the equilibria (26), (27), where  $(x_1, x_2, x_3)$  are the points of the ellipsoid (23).

(ii)  $\alpha \neq 0$ . Then  $y_2 = y_3 = y_4 = 0$  and the condition  $g + F(Y) = 0$  reads

$$y_1^2 - \frac{4}{3}(c_s + 1)y_1 + \frac{4}{3}g = 0,$$

leading to the solutions

$$y_1 = y_{\pm} = \frac{2}{3} \left( (c_s + 1) \pm \sqrt{(c_s + 1)^2 - 3g} \right). \quad (28)$$

Then, the solutions (28) are real when

$$g \leq g_1(c_s) := \frac{1}{3}(c_s + 1). \quad (29)$$

(Note that  $g_1(c_s) < g_2(c_s)$  for all  $c_s > 0$ .) We may summarize the previous analysis as follows.

**Proposition 4.1.** *Let  $c_s > 0$  and  $g_1(c_s), g_2(c_s)$  be given respectively by (29) and (25). The following holds:*

(1) If  $g < g_1(c_s)$  then we have the equilibria

$$\tilde{Y} = (y_{\pm}, 0, 0, 0), \quad (30)$$

$$Y^* = \left( x_3 - \frac{5}{3} \left( c_s + \frac{1}{2} \right), x_1 + \frac{6}{7} x_2, x_3 - \frac{7}{3} \left( c_s + \frac{1}{2} \right), x_2 \right), \quad (31)$$

where  $y_{\pm}$  is given by (28) and  $(x_1, x_2, x_3)$  are the points of the ellipsoid (23).

(2) If  $g = g_1(c_s)$ , then (31) holds and (30) becomes

$$\tilde{Y} = (y_1, 0, 0, 0), \quad y_1 = y_{\pm} = \frac{2}{3} (c_s + 1).$$

(3) If  $g_1(c_s) < g < g_2(c_s)$ , then we just have the equilibria (31).

(4) If  $g = g_2(c_s)$ , then the equilibria (31) reduces to

$$Y^* = \left( -\frac{5}{3} \left( c_s + \frac{1}{2} \right), 0, -\frac{7}{3} \left( c_s + \frac{1}{2} \right), 0 \right),$$

corresponding to  $x_1 = x_2 = x_3 = 0$ .

(5) If  $g > g_2(c_s)$ , then there are no equilibria.

**4.1. The case  $g \leq g_1(c_s)$ .** For  $c_s > 0$  fixed, the present paper is focused on the existence of homoclinic and periodic orbits around the equilibria (30). The first group will correspond to traveling wave (TW) solutions of (13) or (15) approaching  $y_+$  (or  $y_-$ ) when  $t \rightarrow \pm\infty$ . The second group is associated to the existence of periodic traveling wave (PTW) solutions. Note in particular that when  $g = 0$  then

$$y_+ = \frac{2}{3} (c_s + 1), \quad y_- = 0,$$

and those orbits homo-clinic to  $y_-$  at infinity are identified as solitary wave solutions, with the meaning of localized traveling wave solutions.

To this end, our approach will first look for a reduction of (18) to the case  $g = 0$ . Let  $y_{\pm}$  denote any of the equilibria (28). Note that if  $u$  is a solution of (18), then  $\tilde{u} = u - y_{\pm}$  satisfies

$$\begin{aligned} & \left( \frac{3}{2} \mathcal{I} \tilde{u} + \frac{3y_{\pm} - 1}{2} - c_s \right) \tilde{u}'''' + \left( 2c_s + \frac{3 - 5y_{\pm}}{2} \right) \tilde{u}'' + \left( -c_s + \frac{3y_{\pm} - 2}{2} \right) \tilde{u} \\ & \qquad \qquad \qquad = f(\tilde{u}, \tilde{u}', \tilde{u}'', \tilde{u}''') \\ & = \frac{1}{2} \left( -\frac{3}{2} \tilde{u}^2 + \frac{5}{2} (\tilde{u}')^2 + 5\tilde{u}\tilde{u}'' - \frac{9}{2} (\tilde{u}'')^2 - 6\tilde{u}'\tilde{u}''' + 3(\tilde{u}''')^2 \right), \end{aligned} \quad (32)$$

As before, (32) can be written as a first-order system for  $U = (U_1, U_2, U_3, U_4)^T = (\tilde{u}, \tilde{u}', \tilde{u}'', \tilde{u}''')^T$  as

$$\frac{dU}{dZ} = L(c_s, y_{\pm})U + G(U), \quad (33)$$

where

$$L = L(c_s, y_{\pm}) = \begin{pmatrix} 0 & \frac{3y_{\pm} - 1}{2} - c_s & 0 & 0 \\ 0 & 0 & \frac{3y_{\pm} - 1}{2} - c_s & 0 \\ 0 & 0 & 0 & \frac{3y_{\pm} - 1}{2} - c_s \\ c_s + \frac{2 - 3y_{\pm}}{2} & 0 & -(2c_s + \frac{3 - 5y_{\pm}}{2}) & 0 \end{pmatrix},$$

$$G(U) = \begin{pmatrix} \frac{3}{2}U_2(U_1 - U_3) \\ \frac{3}{2}U_3(U_1 - U_3) \\ \frac{3}{2}U_4(U_1 - U_3) \\ \tilde{F}(U) \end{pmatrix},$$

$$\tilde{F}(U) = -\left(\frac{9}{4}U_3^2 - \frac{5}{2}U_1U_3\right) - \frac{3}{4}U_1^2 + \frac{5}{4}U_2^2 - 3U_2U_4 - \frac{3}{2}U_4^2.$$

The structure of solutions of (13) or (15) around  $y_{\pm}$  can be analyzed from that of solutions of (33) around  $U = 0$ . Since  $G(0) = G'(0) = 0$ , then, if we first linearize, the characteristic polynomial of  $L$  is of the form  $z^4 - bz^2 + a$ , where

$$a = a_{\pm} = -\beta_{\pm}\alpha_{\pm}^3, \quad b = b_{\pm} = -\alpha_{\pm}\gamma_{\pm},$$

$$\alpha_{\pm} = \frac{3y_{\pm} - 1}{2} - c_s, \quad \beta_{\pm} = c_s + \frac{2 - 3y_{\pm}}{2}, \quad \gamma_{\pm} = 2c_s + \frac{3 - 5y_{\pm}}{2}, \quad (34)$$

We note that (33) is reversible with respect to the transformation

$$S : (U_1, U_2, U_3, U_4) \mapsto (U_1, -U_2, U_3, -U_4),$$

in the sense that, [18]

$$SLU = -LSU, \quad SG(U) = -G(SU).$$

This implies that the linear dynamics around  $U = 0$  follows Figure 1, [9], in the  $(b, a)$  plane. Four regions of different dynamics are determined from the four curves

$$\begin{aligned} \mathbb{C}_0 &= \{(b, a)/a = 0, b > 0\}, \\ \mathbb{C}_1 &= \{(b, a)/a = 0, b < 0\}, \\ \mathbb{C}_2 &= \{(b, a)/a > 0, b = -2\sqrt{a}\}, \\ \mathbb{C}_3 &= \{(b, a)/a > 0, b = 2\sqrt{a}\}. \end{aligned} \quad (35)$$

On the curve  $\mathbb{C}_0$  there are two zero eigenvalues and two real; on  $\mathbb{C}_1$  there are two zero eigenvalues and two imaginary; on  $\mathbb{C}_2$  there is a double complex conjugate pair of imaginary eigenvalues  $\pm i\sqrt{|b|/2}$ , and on  $\mathbb{C}_3$  there are two double real eigenvalues  $\pm\sqrt{b/2}$ , symmetric with respect to the imaginary axis. The spectrum of  $L$  in the regions delimited by the four curves is represented schematically in Figure 1.

The existence of different types of orbits in each region and with respect to each equilibrium in (28) is analyzed using two approaches. The first one is theoretical and is based on the Normal Form theory and the theory of reversible bifurcations, cf. e. g. [18], as well as the study of the corresponding systems derived from a center manifold reduction. But the discussion will be also strongly supported by numerical simulations. To this end, a numerical procedure to approximate solutions of (32) is implemented. This is described in Appendix A.

**4.2. Some previous lemmas.** The analysis below will require some previous results concerning the coefficients (34) and new relevant values of the constant  $g$ . We note first that when  $g \leq g_1(c_s)$  then  $0 \leq y_- \leq y_+$ . Furthermore, it is not hard to prove the following result.

**Lemma 4.2.** *Let  $c_s > 0$  and assume that  $g \leq g_1(c_s)$ . we define*

$$g_1^*(c_s) := g_1(c_s) - \frac{1}{75} \left(c_s - \frac{1}{2}\right)^2, \quad g_1^{**}(c_s) := g_1(c_s) - \frac{1}{12}. \quad (36)$$

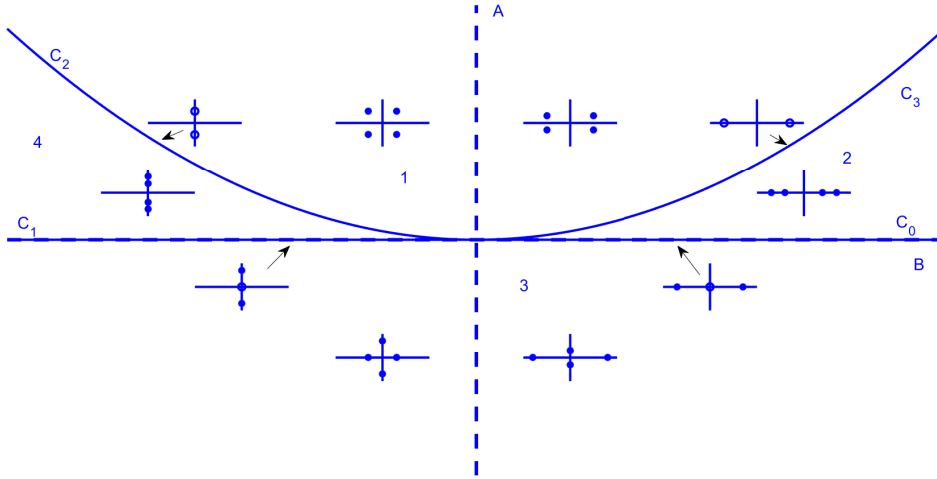


FIGURE 1. Linearization at the origin of (33) (cf. [9, Figure 1]): Regions 1 to 4 in the  $(b, a)$ -plane, delimited by the bifurcation curves  $C_0$  to  $C_3$  given by (35), and schematic representation of the position in the complex plane of the eigenvalues of  $L$  for each curve and region. (Dot: simple root, larger dot: double root.)

Then it holds that:

- (1)  $\alpha_+ > 0, \beta_+ \leq 0, \beta_- \geq 0$ .
- (2)  $\alpha_- \geq 0 \Leftrightarrow g \geq g_1^{**}(c_s)$ .
- (3)  $\gamma_+ > 0 \Leftrightarrow c_s > \frac{1}{2}$  and  $g > g_1^*(c_s)$ .
- (4)  $\gamma_- > 0 \Leftrightarrow c_s \geq \frac{1}{2}$  and  $g < g_1^*(c_s)$  when  $c_s < \frac{1}{2}$ .

In addition, for each case  $y_+, y_-$ , we will need to identify the position of the roots of characteristic polynomial of  $L$  in the  $(b, a)$  plane from the sign of the coefficients  $a_{\pm}, b_{\pm}$  and  $\Delta_{\pm} = b_{\pm}^2 - 4a_{\pm}$ . After some computations, we observe that

$$\begin{aligned} \Delta_{\pm} &= \alpha_{\pm}^2 S_{\pm}, \\ S_{\pm} &= \gamma_{\pm}^2 + 4\alpha_{\pm}\beta_{\pm} = -\frac{11}{9}(\beta_{\pm} - \delta_+)(\beta_{\pm} - \delta_-), \\ \delta_{\pm} &= \frac{1}{22} \left( (10c_s + 13) \pm \sqrt{(10c_s + 13)^2 + 44 \left( c_s - \frac{1}{2} \right)^2} \right), \end{aligned}$$

with  $\delta_- < 0 < \delta_+$  for  $c_s > 0$ . This leads to the following properties:

**Lemma 4.3.** *Let  $c_s > 0$  and assume that  $g \leq g_1(c_s)$ . We define*

$$g_-(c_s) := g_1(c_s) - \frac{1}{3}\delta_-^2, \quad g_+(c_s) := g_1(c_s) - \frac{1}{3}\delta_+^2. \quad (37)$$

Then:

- (i)  $\Delta_+ > 0 \Leftrightarrow g > g_-(c_s)$ .
- (ii) If  $g_1^{**}(c_s) < g < g_1(c_s)$  then  $\Delta_- > 0$ . When  $g < g_1^{**}(c_s)$  then

$$\Delta_- > 0 \Leftrightarrow g > g_+(c_s).$$

A final result compares the limiting values of  $g$  appearing above and in Lemma 4.2 and it is illustrated in Figure 2.

**Lemma 4.4.** *Let  $c_s > 0$  and assume that  $g \leq g_1(c_s)$ .*

- (1)  $g_+(c_s) < 0 < g_-(c_s)$  and  $g_1^*(c_s), g_1^{**}(c_s) > 0$ .
- (2)  $g_1^*(c_s) < g_-(c_s)$  and  $g_1^{**}(c_s) \leq g_-(c_s) \Leftrightarrow c_s \leq 3(1 + \sqrt{2})$ .
- (3)  $g_1^*(c_s) \leq g_1^{**}(c_s) \Leftrightarrow c_s \geq 3$ ,

where  $g_1^*(c_s), g_1^{**}(c_s)$  and  $g_+(c_s), g_-(c_s)$  are given by (36) and (37), respectively.

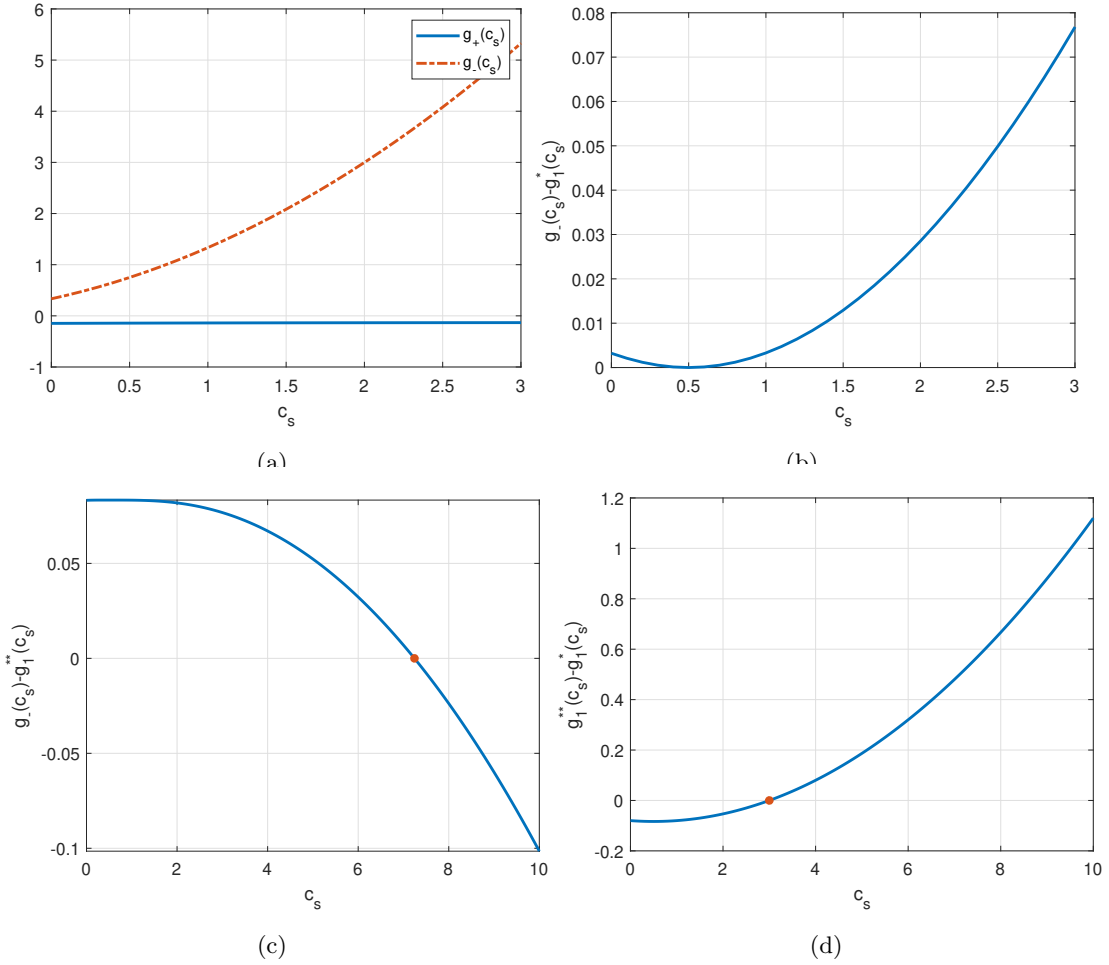


FIGURE 2. Illustration of Lemma 4.4. (a), (b) Case (1); (c) Case (2), where the remarked dot corresponds to  $c_s = 3(1 + \sqrt{2})$ ; (d) Case (c), where the remarked dot corresponds to  $c_s = 3$

## 5. EXISTENCE OF NON-PERIODIC TRAVELING WAVE SOLUTIONS

Making use of Lemmas 4.2-4.4, we will study the dynamics of (33) with respect to each of the equilibria (28)

5.1. **Dynamics around the equilibrium  $y_+$ .** The analysis for the equilibrium  $y_+$  leads to the following situations:

- (i) Assume that  $c_s > \frac{1}{2}$ . In that case,  $a_+ > 0$  and we have three possibilities:
  - (i1) If  $g < g_1^*(c_s)$ , then  $b_+ > 0$  and  $\Delta_+ < 0$ . The linearization matrix  $L(c_s, y_+)$  has two symmetric couples of complex conjugate eigenvalues (region 1, right of Figure 1). Here the dynamics can be analyzed following the approach made in, e. g. [11]. The numerical computations suggest the generation of classical traveling waves of depression with a nonmonotone behaviour. For  $g$  close to  $g_1^*(c_s)$ , the profiles are smooth (cf. Figure 3), developing some kind of peak at the point of maximum negative excursion as  $g$  separates from  $g_1^*(c_s)$ .
  - (i2) When  $g_1^*(c_s) \leq g < g_-(c_s)$ , then  $b_+ < 0$  and  $\Delta_+ < 0$ . The spectrum of the linearization corresponds to region 1, left, of Figure 1. In Figure 4, it is shown the persistence of the generation of classical traveling waves (of depression) with nonmonotone asymptotic behaviour. Note that as  $g \rightarrow g_-(c_s)$  then  $\Delta_+ \rightarrow 0$  and we fall into the curve  $\mathbb{C}_2$ , where the spectrum of the linearization changes to a double complex conjugate pair of imaginary eigenvalues. This seems to be reflected by a more oscillatory approach towards the equilibrium  $y_+$  as  $Z \rightarrow \pm\infty$ , [9,14], see Figure 5.
  - (i3) When  $g_-(c_s) \leq g < g_1(c_s)$ , then  $b_+ < 0$  and  $\Delta_+ > 0$  (region 4 of Figure 1, where the spectrum has four imaginary eigenvalues, two by two conjugate). The behaviour of the orbits as  $g \rightarrow g_-$ , described above, and the numerical computations (cf. Figure 6) suggest that crossing from region 1 (left) to region 4 forms a bifurcation that may change the dynamics from the generation of nonmonotone traveling waves to periodic orbits in the form of periodic traveling waves, [20]. As  $g$  approaches  $g_1(c_s)$ , we are approximating to the curve  $\mathbb{C}_1$ , where the spectrum consists of two zero eigenvalues and two imaginary. The computations do not detect any modification in the nature of the generated profiles, although the amplitude of the emerging periodic traveling waves seems to decrease to zero and the solution tends to the constant state  $y_+$ .
- (ii) Assume that  $c_s < \frac{1}{2}$ . In that case,  $a_+ > 0$ ,  $b_+ > 0$  (since  $\gamma_+ < 0$ ) and we may have two possibilities:
  - (ii1) If  $g < g_-(c_s)$  then  $\Delta_+ < 0$  and this corresponds to region 1, right of Figure 1: the linearization matrix  $L(c_s, y_+)$  has four (symmetric) complex eigenvalues. The results are then similar to those obtained in (i1), where the homo-clinic orbits correspond to nonmonotone classical traveling waves. In this case, the profiles seem to be more regular as  $g$  approaches  $g_-(c_s)$  (cf. Figures 7 and 8).
  - (ii2) If  $g_-(c_s) \leq g < g_1(c_s)$  then  $\Delta_+ > 0$  and we fall into region 2 of Figure 1. When crossing from region 1 to region 2 and  $g$  goes from  $g_-$  to  $g_1$  (approaching the curve  $\mathbb{C}_0$ ) there seems to be a change of type of homo-clinic orbit (cf Figures 9 and 10) with the generation of classical traveling waves with a monotone asymptotic behaviour towards  $y_+$ , [20].

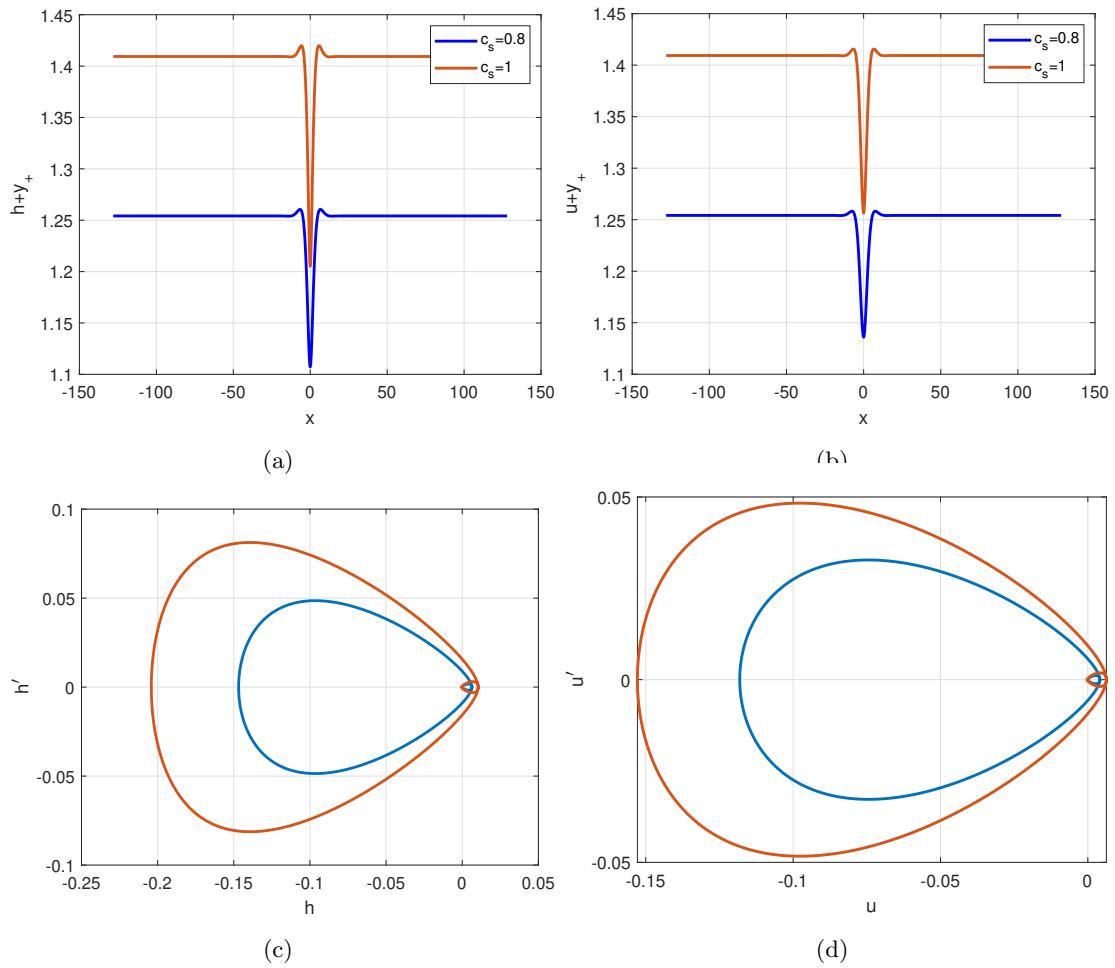


FIGURE 3. Approximations to traveling-wave solutions of (16) for two values of  $c_s$ . Case  $g = g_1^*(c_s) - 0.001$ . (a)  $\tilde{h} + y_+$  profile; (b)  $\tilde{u} + y_+$  profile; (c)  $\tilde{h}$  phase plot; (d)  $\tilde{u}$  phase plot.

The results are summarized in Table 1.

$c_s > \frac{1}{2}(a_+ > 0)$	$(b, a)$ region	Type of wave
$g < g_1^*(c_s)$	1R	NMTW (dep.)
$g_1^*(c_s) \leq g < g_-(c_s)$	1L	NMTW (dep.)
$g_-(c_s) \leq g < g_1(c_s)$	4	PTW
$c_s < \frac{1}{2}(a_+ > 0)$	$(b, a)$ region	Type of wave
$g < g_-(c_s)$	1R	NMTW (dep.)
$g_-(c_s) \leq g < g_1(c_s)$	2	MTW (dep.)

TABLE 1. Bifurcation study of homo-clinic orbits around the equilibrium  $y_+$ . NMTW (dep.): Nonmonotone traveling wave of depression; MTW: Monotone traveling wave of depression; PTW: Periodic traveling wave.

**5.2. Dynamics around the equilibrium  $y_-$ .** A similar study for the equilibrium  $y_-$  leads to the following results.



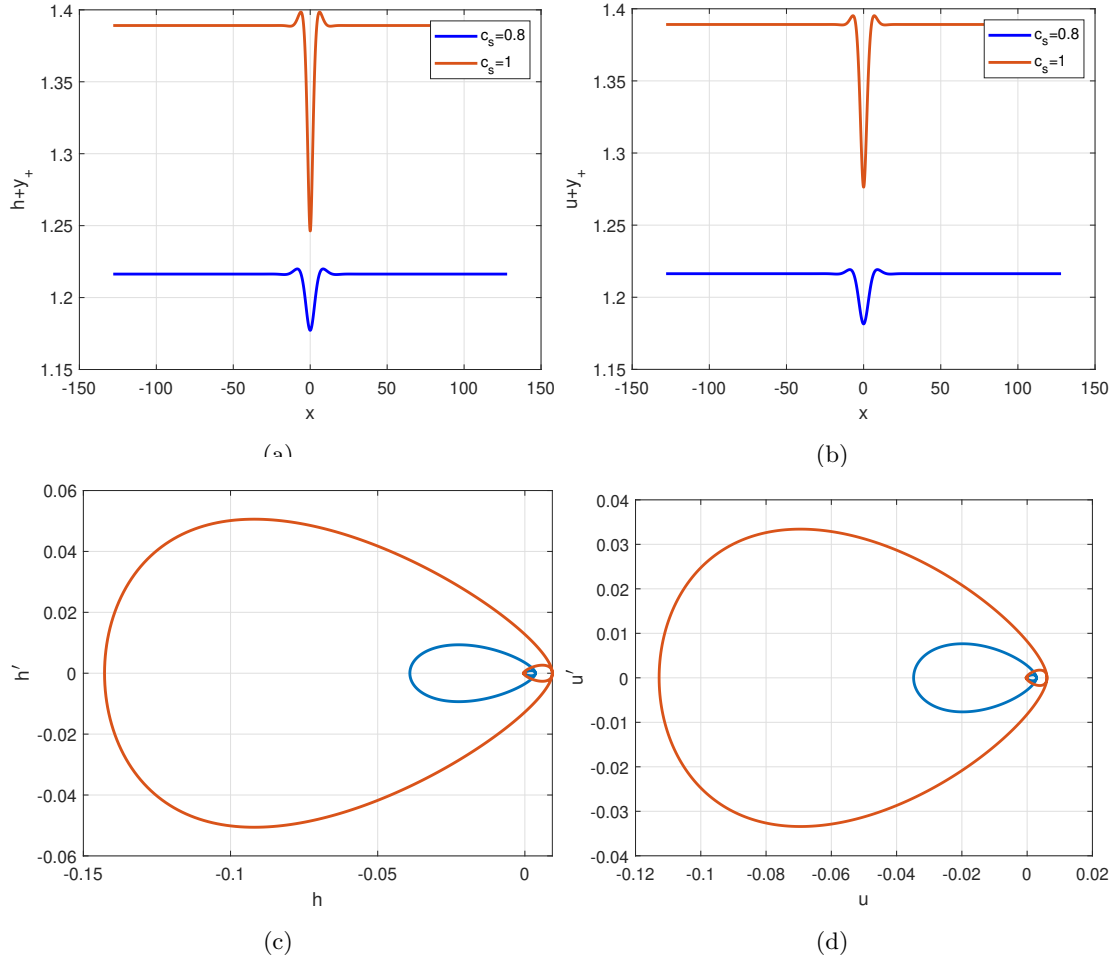


FIGURE 4. Approximations to traveling-wave solutions of (16) for two values of  $c_s$ . Case  $g = g_1^*(c_s) + 0.001$ . (a)  $\tilde{h} + y_+$  profile; (b)  $\tilde{u} + y_+$  profile; (c)  $\tilde{h}$  phase plot; (d)  $\tilde{u}$  phase plot.

- (i)  $c_s < \frac{1}{2}$ . Here we may have four situations:
- (i1)  $g < g_+(c_s)$ . Then  $a_-, b_- > 0$ , and  $\Delta_- < 0$ . Region 1, right.
  - (i2)  $g_+(c_s) \leq g < g_1^{**}(c_s)$ . Then  $a_-, b_- > 0$ , and  $\Delta_- > 0$ . Region 2.
  - (i3)  $g_1^{**}(c_s) \leq g < g_1^*(c_s)$ . Then  $a_-, b_- < 0$ , and  $\Delta_- > 0$ . Region 3, left.
  - (i4)  $g_1^*(c_s) \leq g < g_1(c_s)$ . Then  $a_- < 0, b_- > 0$ , and  $\Delta_- > 0$ . Region 3, right.
- (ii)  $\frac{1}{2} < c_s < \frac{3}{2}$ . Here we may have four situations:
- (ii1)  $g < g_+(c_s)$ . Then  $a_-, b_- > 0$ , and  $\Delta_- < 0$ . Region 1, right.
  - (ii2)  $g_+(c_s) \leq g < g_1^{**}(c_s)$ . Then  $a_-, b_- > 0$ , and  $\Delta_- > 0$ . Region 2.
  - (ii3)  $g_1^{**}(c_s) \leq g < g_1^*(c_s)$ . Then  $a_-, b_- < 0$ , and  $\Delta_- > 0$ . Region 3, left.
  - (ii4)  $g_1^*(c_s) \leq g < g_1(c_s)$ . Then  $a_- < 0, b_- < 0$ , and  $\Delta_- > 0$ . Region 3, left.
- (iii)  $c_s > \frac{3}{2}$ . Here we may have four situations:
- (iii1)  $g < g_+(c_s)$ . Then  $a_-, b_- > 0$ , and  $\Delta_- < 0$ . Region 1, right.
  - (iii2)  $g_+(c_s) \leq g < g_1^*(c_s)$ . Then  $a_-, b_- > 0$ , and  $\Delta_- > 0$ . Region 2.
  - (iii3)  $g_1^*(c_s) \leq g < g_1^{**}(c_s)$ . Then  $a_-, b_- > 0$ , and  $\Delta_- > 0$ . Region 2.

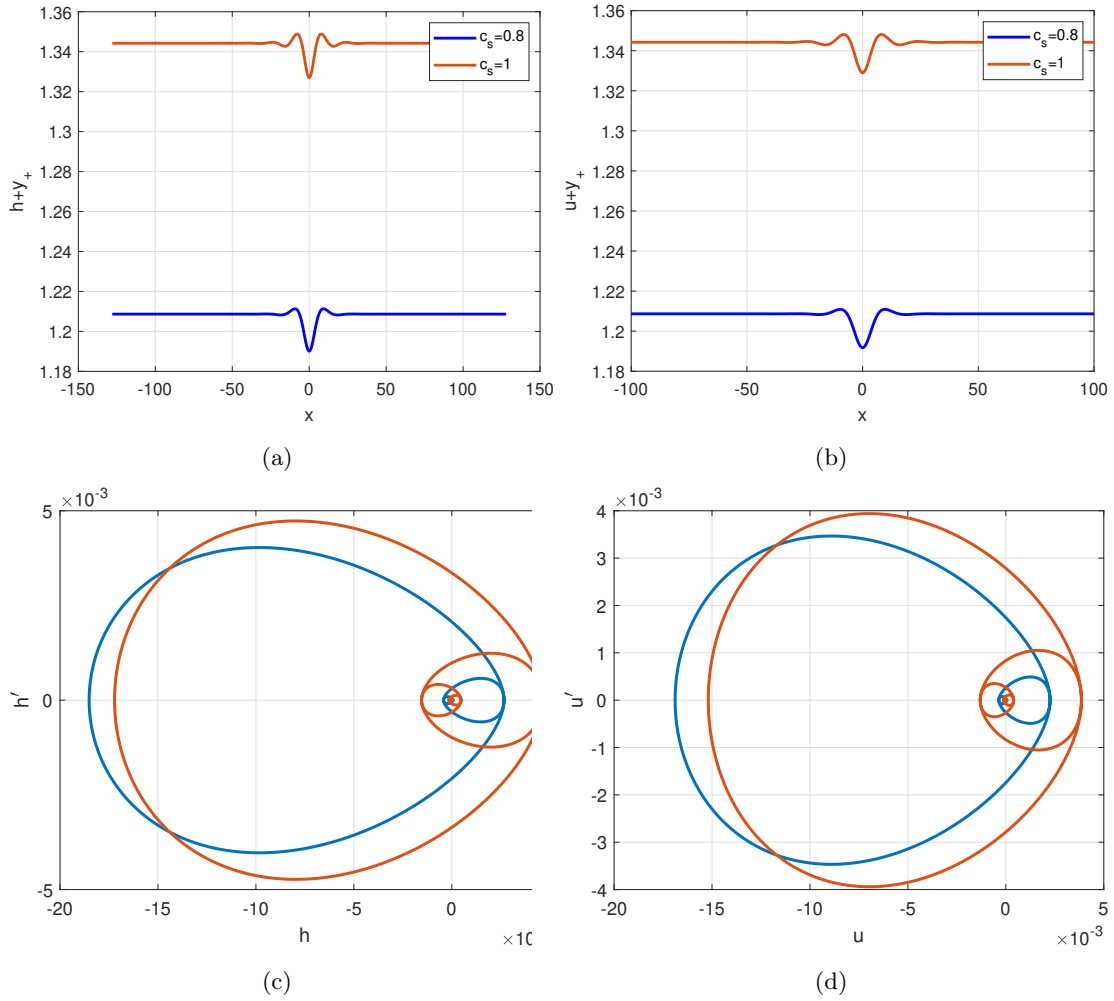


FIGURE 5. Approximations to traveling-wave solutions of (16) for two values of  $c_s$ . Case  $g = g_-(c_s) - 10^{-4}$ . (a)  $\tilde{h} + y_+$  profile; (b)  $\tilde{u} + y_+$  profile; (c)  $\tilde{h}$  phase plot; (d)  $\tilde{u}$  phase plot.

(iii4)  $g_1^*(c_s) \leq g < g_1(c_s)$ . Then  $a_- < 0, b_- < 0$ , and  $\Delta_- > 0$ . Region 3, left.

The types of the generated profiles corresponding to the homo-clinic orbits with limit at  $y_-$  are summarized in Table 2. Compared to Table 1, several differences can be mentioned:

- The types of the emerging traveling waves in the regions do not depend on the range (i), (ii) or (iii) of the speed  $c_s$ .
- The non-periodic computed traveling waves are now of elevation.
- In regions 1, right, and 2, classical traveling waves (of elevation) are computed. The  $h$  and  $u$  profiles seem to have a non-monotone behaviour (more clearly observed in the first case) which seems to evolve to a monotone decay to the equilibrium  $y_-$  as  $g$  approaches  $g_+(c_s)$ , cf. Figure 11. (Thus,  $(b_-, a_-)$  is closer to the curve  $\mathbb{C}_3$  and eventually crosses from region 1, right, to region 2.) The profiles develop a peak at the point where the maximum is attained, which is more pronounced and larger for larger speeds, as observed in Figure 12. Note in this case that  $y_- = 0$ , and the computed traveling waves are solitary

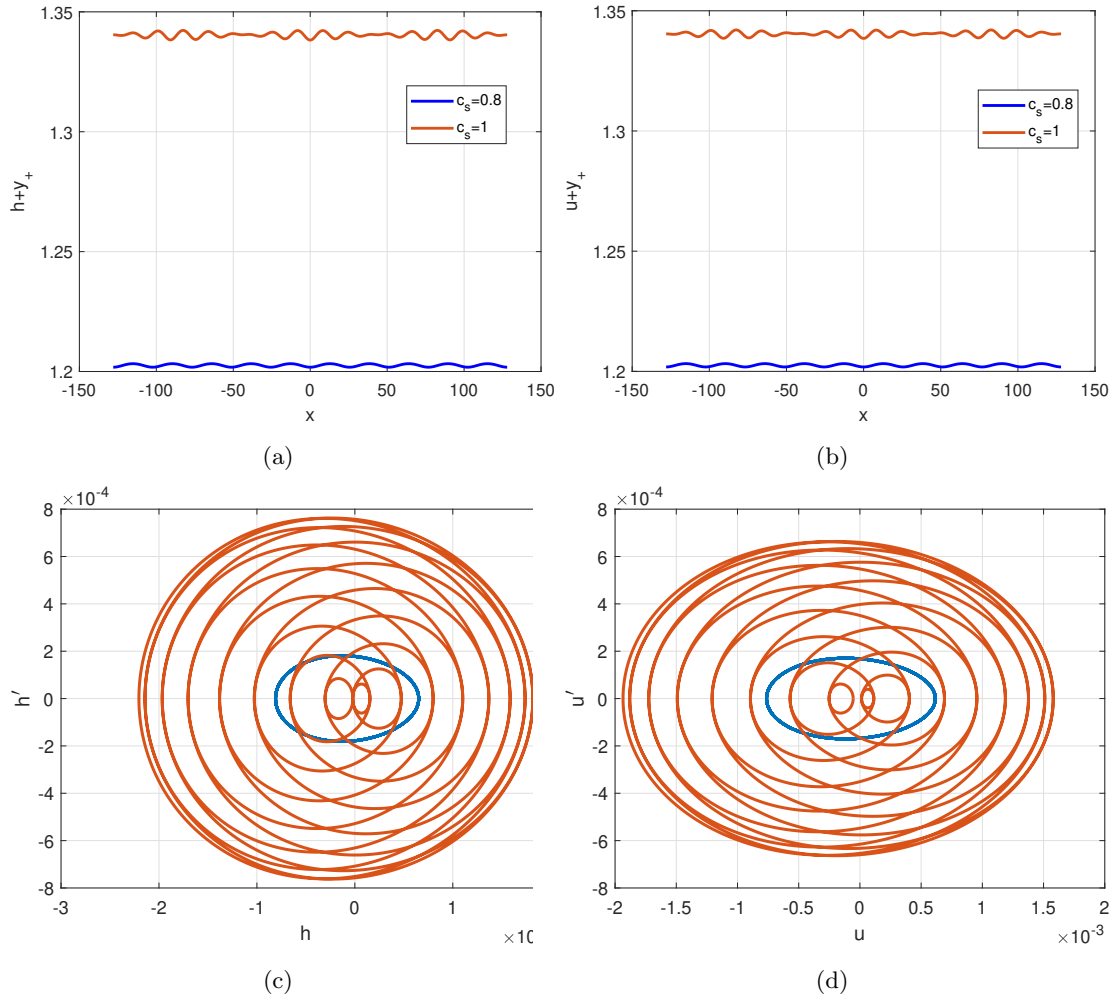


FIGURE 6. Approximations to traveling-wave solutions of (16) for two values of  $c_s$ . Case  $g = g_-(c_s) + 10^{-6}$ . (a)  $\tilde{h} + y_+$  profile; (b)  $\tilde{u} + y_+$  profile; (c)  $\tilde{h}$  phase plot; (d)  $\tilde{u}$  phase plot.

waves. A more rigorous proof of existence of such solitary waves may be considered by using classical approaches such as the concentration compactness theory of Lions, [26], or the positive operator theory, [6].

- Crossing from region 2 to region 3 (left) generates a change from computed classical traveling waves to periodic traveling waves, see Figure 13. PTW's are also computed in region 3, right.

## 6. CONCLUDING REMARKS

The present paper is concerned with the existence of traveling wave solutions of the asymptotic model (4) for the evolution of a collision-free plasma in a magnetic field. In Section 3, using Crandall-Rabinowitz theorem [13] and the ideas in [2], we can rigorously prove the existence of traveling waves of small amplitude for (4).

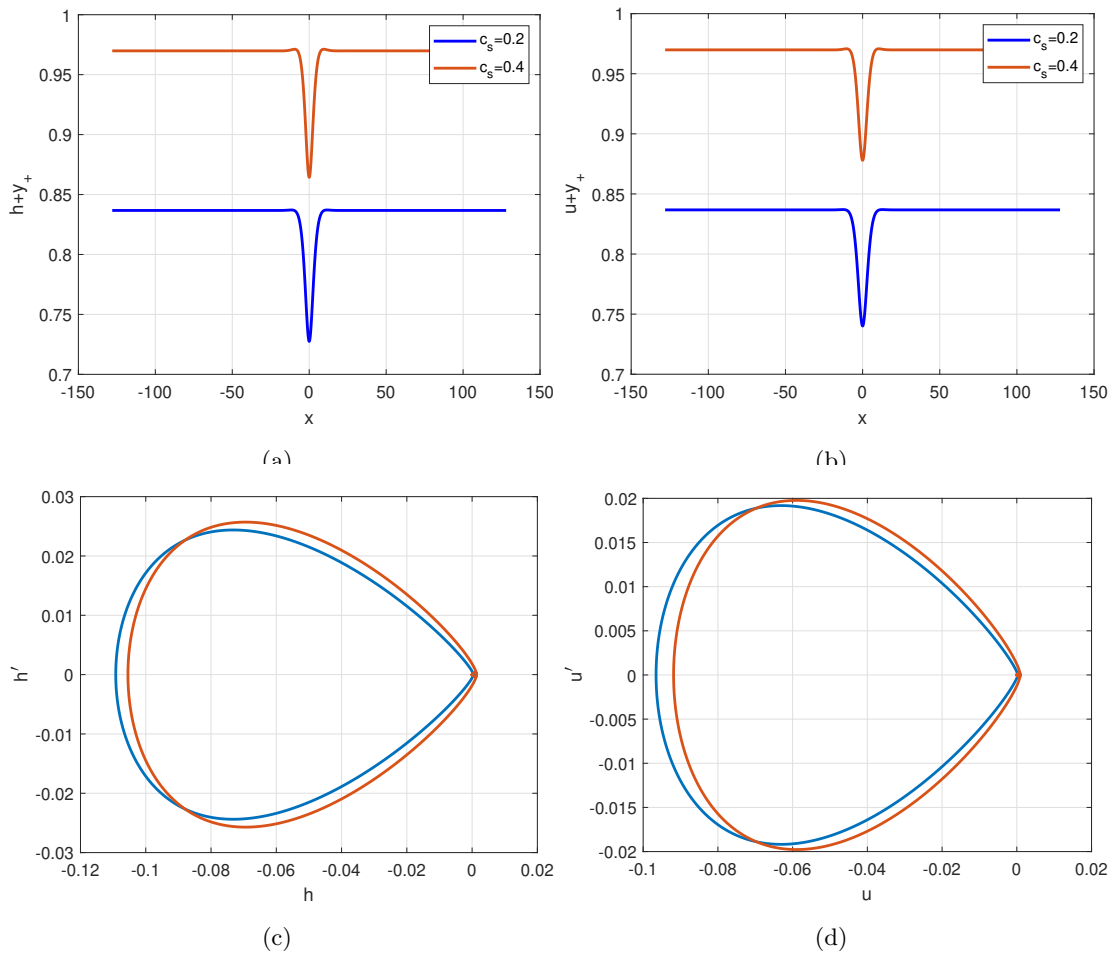


FIGURE 7. Approximations to traveling-wave solutions of (16) for two values of  $c_s$ . Case  $g = g_-(c_s) - 0.001$ . (a)  $\tilde{h} + y_+$  profile; (b)  $\tilde{u} + y_+$  profile; (c)  $\tilde{h}$  phase plot; (d)  $\tilde{u}$  phase plot.

Furthermore, from a reformulation of the model which involves only local terms, the corresponding ode system for the profiles of the traveling wave solutions is derived and the existence of equilibria is discussed in terms of the speed of the wave and a constant of integration  $g$ , playing the rôle of bifurcation parameter. The structure of solutions around two of these equilibria can be studied from that of the solutions of an equivalent first-order system (33) around the origin as equilibrium. The reversible character of the system enables to analyze the dynamics from the application of normal form theory for reversible vector fields, [18], in related references, [9–11]. With this approach, and supported by an efficient numerical code to generate computed traveling wave profiles (described in Appendix A), the emergence of several traveling waves is revealed. The classification depends on the speed on the waves and the constant  $g$  as bifurcation parameter. The types of traveling wave solutions include classical traveling waves of monotone and non-monotone behaviour, classical solitary waves (localized traveling waves) and periodic traveling waves. In addition, some experiments suggest the convergence of peakon-type waves, cf. [31].

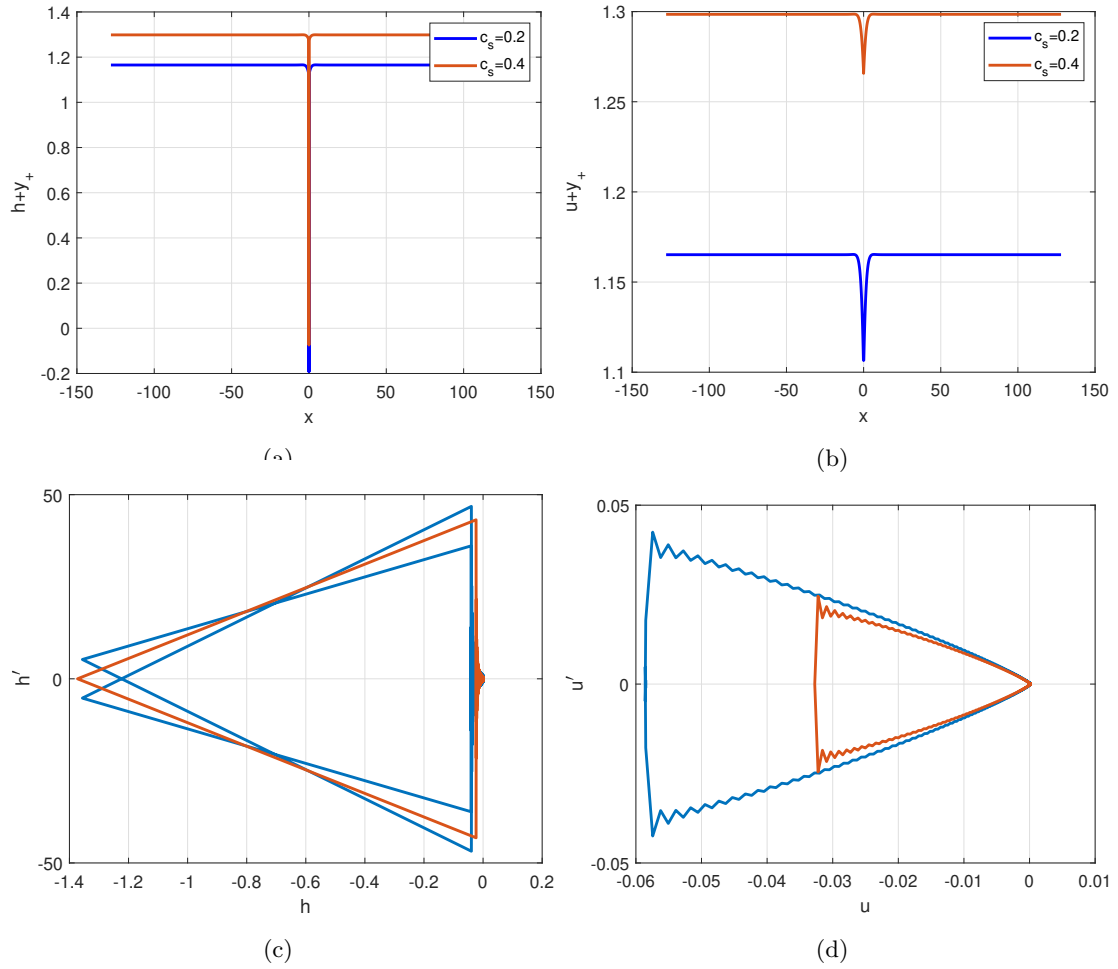


FIGURE 8. Approximations to traveling-wave solutions of (16) for two values of  $c_s$ . Case  $g = g_-(c_s) - 0.001$ . (a)  $\tilde{h} + y_+$  profile; (b)  $\tilde{u} + y_+$  profile; (c)  $\tilde{h}$  phase plot; (d)  $\tilde{u}$  phase plot.

## REFERENCES

- [1] H. Abels *Pseudo-differential and Singular Integral Operators: An Introduction with Applications*. Berlin, Boston: De Gruyter, (2012), <https://doi.org/10.1515/9783110250312>
- [2] D. Alonso-Orán, C. García, R. Granero-Belinchón. *Traveling gravity-capillary waves with odd viscosity*. arXiv preprint [arXiv:2407.19743](https://arxiv.org/abs/2407.19743), (2024).
- [3] D. Alonso-Orán, A. Durán, R. Granero-Belinchón, *Derivation and well-posedness for asymptotic models of cold plasmas*, *Nonlinear Anal.*, 244 (2024) 113539.
- [4] D. Alonso-Orán, R. Granero-Belinchón, *Well-posedness for an hyperbolic-hyperbolic-elliptic system describing cold plasmas*, *Applied Mathematics Letters*, 147, (2024).
- [5] J. Bae, J. Choi and B. Kwon, *Singularity formation of hydromagnetic waves in cold plasma*, [arXiv:2407.18619](https://arxiv.org/abs/2407.18619), (2024).
- [6] T.B. Benjamin, J.L. Bona, D.K. Bose, *Solitary-wave solutions of nonlinear problems*, *Philos. Trans. Royal Soc. London A* 331 (1990), 195-244.
- [7] C. Canuto, M. Y. Hussaini, A. Quarteroni, A. T. Zang, *Spectral Methods in Fluid Dynamics*, Springer, New York, (1985).

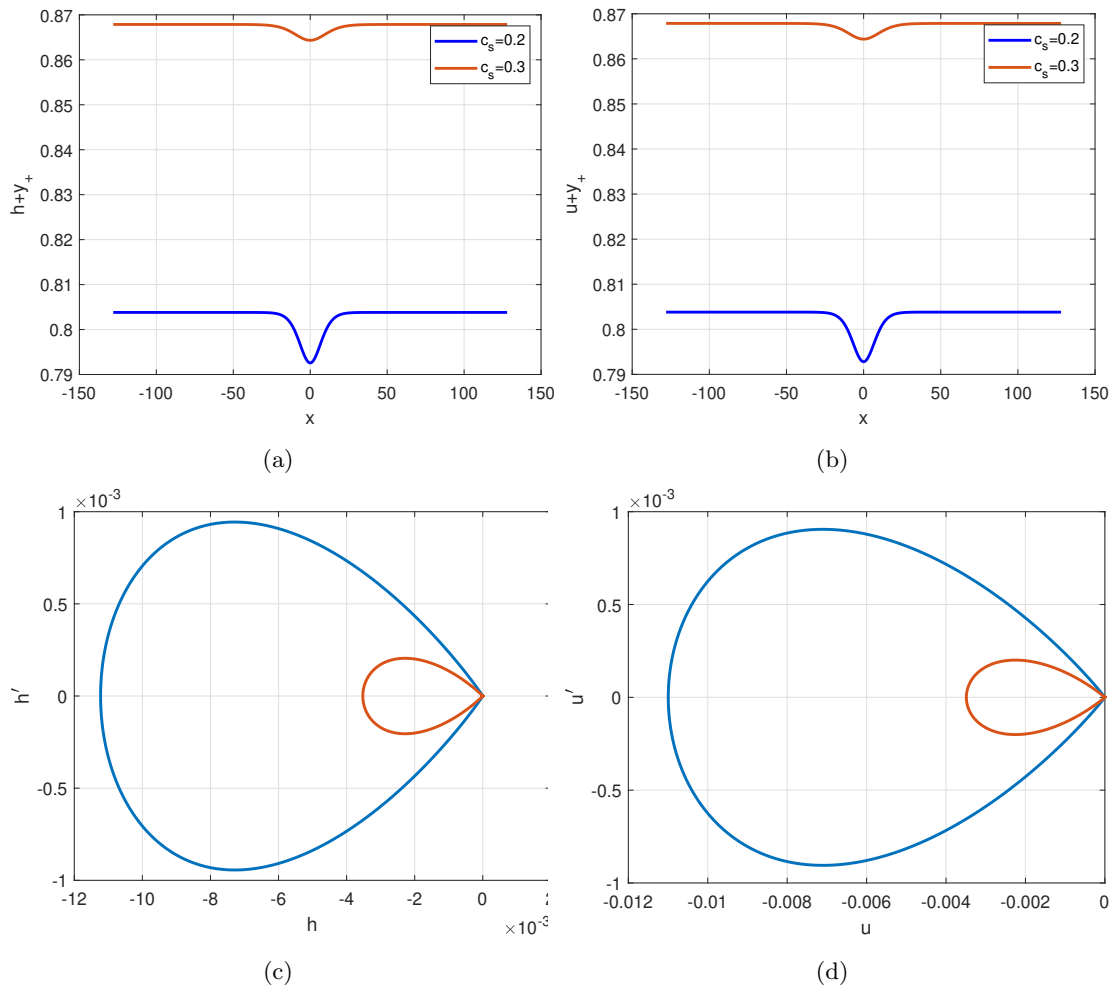


FIGURE 9. Approximations to traveling-wave solutions of (16) for two values of  $c_s$ . Case  $g = g_-(c_s) + 10^{-6}$ . (a)  $\tilde{h} + y_+$  profile; (b)  $\tilde{u} + y_+$  profile; (c)  $\tilde{h}$  phase plot; (d)  $\tilde{u}$  phase plot.

- [8] Y. A. Berezin, V. Karpman, *Theory of nonstationary finite-amplitude waves in a low-density plasma*, Sov. Phys. JETP 19 1265–1271 (1964).
- [9] A. R. Champneys, *homo-clinic orbits in reversible systems and their applications in mechanics, fluids and optics*, Physica D, 112, 158-186, (1988).
- [10] A. R. Champneys, A. Spence, *Hunting for homo-clinic orbits in reversible systems: A shooting technique*, Adv. Comput. Math., 1 81-108, (1993).
- [11] A.R. Champneys, J.F. Toland, *Bifurcation of a plethora of multi-modal homo-clinic orbits for autonomous Hamiltonian systems*, Nonlinearity 6, 665-772, (1993).
- [12] A. Constantin and E. Varvaruca, *Steady periodic water waves with constant vorticity: regularity and local bifurcation*. Arch. Rational Mech. Anal., 199, pp. 33–67, (2011).
- [13] M. G. Crandall and P. H. Rabinowitz, *Bifurcation from simple eigenvalues*. Journal of Functional Analysis, 8, pp. 321–340, (1971).
- [14] V. A. Dougalis, A. Durán, D. E. Mitsotakis, *Numerical approximation of solitary waves of the Benjamin equation*, Math. Comp. Simul., 127 56-79, (2016).
- [15] V. A. Dougalis, A. Durán, L. Saridaki, *On solitary-wave solutions of Boussinesq/Boussinesq systems for internal waves*, Physica D, 428, 133051, (2021).

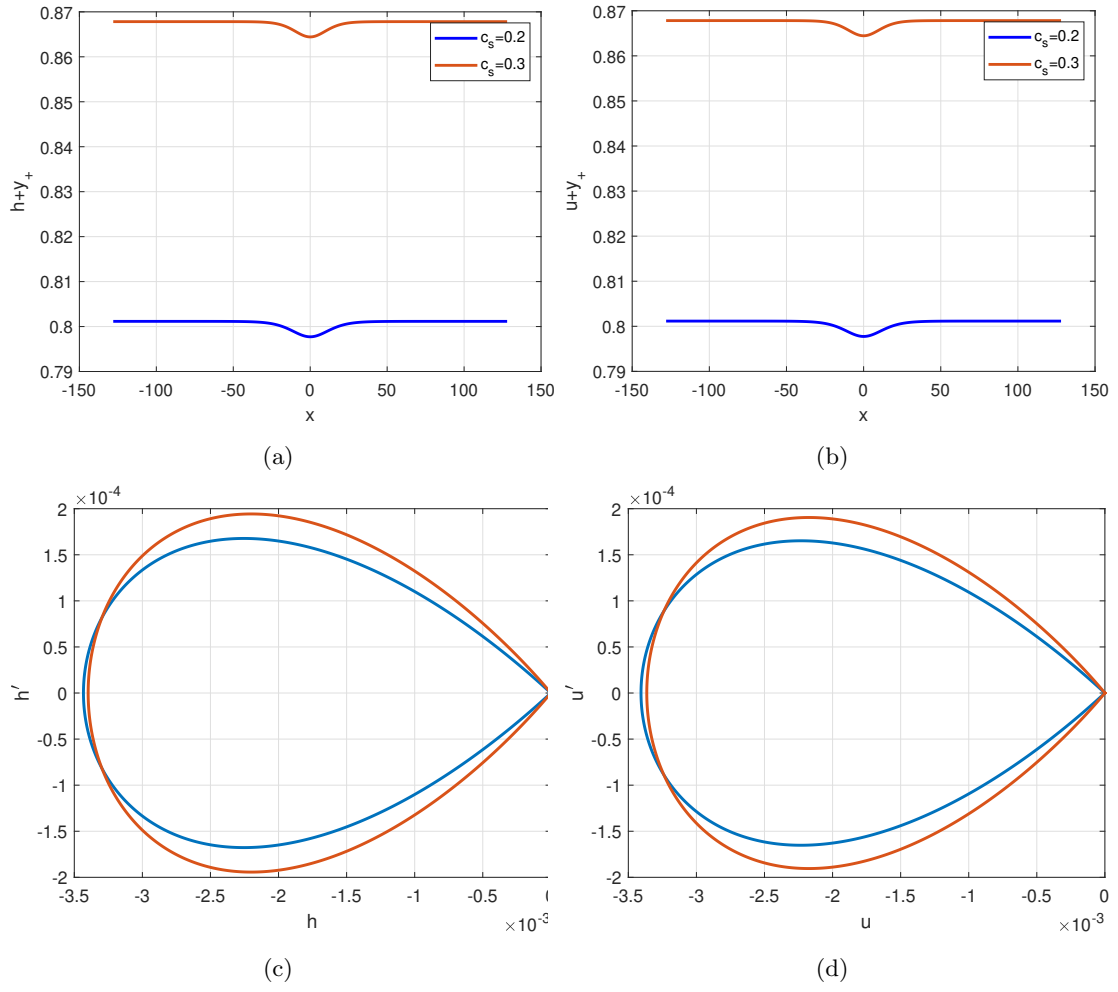


FIGURE 10. Approximations to traveling-wave solutions of (16) for two values of  $c_s$ . Case  $g = g_1(c_s) - 10^{-6}$ . (a)  $\tilde{h} + y_+$  profile; (b)  $\tilde{u} + y_+$  profile; (c)  $\tilde{h}$  phase plot; (d)  $\tilde{u}$  phase plot.

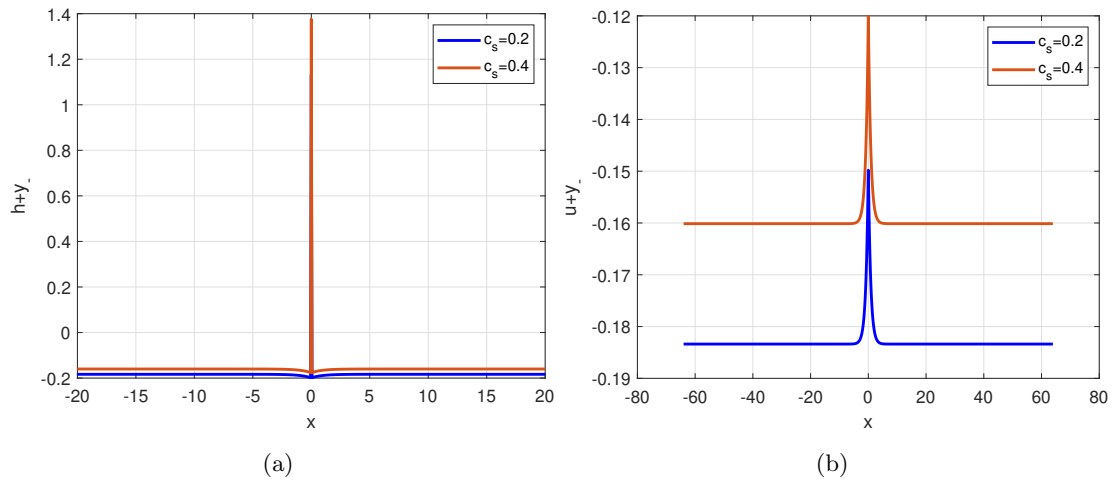


FIGURE 11. Approximations to traveling-wave solutions of (16) for two values of  $c_s$ . Case  $g = g_+(c_s) - 0.1$ . (a)  $\tilde{h} + y_-$  profile; (b)  $\tilde{u} + y_-$  profile.

$c_s < \frac{1}{2}$	$(b, a)$ region	Type of wave
$g < g_1^+(c_s)$	1R	TW (el.)
$g_+(c_s) \leq g < g_1^{**}(c_s)$	2	TW (el.)
$g_1^{**}(c_s) \leq g < g_1^*(c_s)$	3L	TW-PTW
$g_1^*(c_s) \leq g < g_1(c_s)$	3R	PTW
$\frac{1}{2} < c_s < \frac{3}{2}$	$(b, a)$ region	Type of wave
$g < g_+(c_s)$	1R	TW (el.)
$g_+(c_s) \leq g < g_1^{**}(c_s)$	2	TW (el.)
$g_1^{**}(c_s) \leq g < g_1^*(c_s)$	3L	TW-PTW
$g_1^*(c_s) \leq g < g_1(c_s)$	3L	TW-PTW
$c_s > \frac{3}{2} (a_+ > 0)$	$(b, a)$ region	Type of wave
$g < g_+(c_s)$	1R	TW (el.)
$g_+(c_s) \leq g < g_1^*(c_s)$	2	TW (el.)
$g_1^*(c_s) \leq g < g_1^{**}(c_s)$	2	TW (el.)
$g_1^{**}(c_s) \leq g < g_1(c_s)$	3L	TW-PTW

TABLE 2. Bifurcation study of homo-clinic orbits around the equilibrium  $y_-$  TW (el.): Traveling waves of elevation; PTW: Periodic traveling waves.

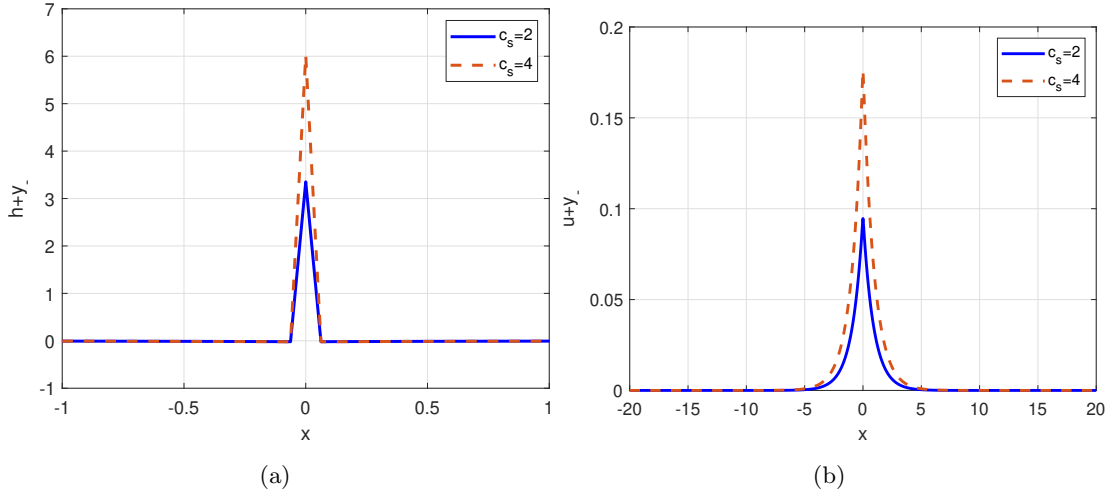


FIGURE 12. Approximations to traveling-wave solutions of (16) for two values of  $c_s$ . Case  $g = 0$ . (a)  $\tilde{h} + y_-$  profile; (b)  $\tilde{u} + y_-$  profile.

- [16] V. A. Dougalis, A. Durán, L. Saridaki, *Numerical solution of internal-wave systems in the intermediate long wave and the Benjamin-Ono regimes*, Bull. Hellenic Math. Soc., 66,11–25, (2022).
- [17] C. Gardner, G. Morikawa, *Similarity in the asymptotic behaviour of collision-free hydromagnetic waves and water waves*, Tech. rep., New York Univ., New York. Inst. of Mathematical Sciences (1960).
- [18] M. Haragus, G. Iooss, *Local Bifurcations, Center Manifolds, and Normal Forms in Infinite-Dimensional Dynamical Systems*, Springer London Dordrecht Heidelberg New York, (2011).
- [19] G. Iooss, M. Adelmeyer, *Topics in Bifurcation Theory and Applications*, 2nd ed., World Scientific, Singapore, (1999).
- [20] G. Iooss, K. Kirchgässner, *Water waves for small surface tension: an approach via normal form*, Proc. Roy. Soc. Edinburgh A 112 267-200, (1992).
- [21] T. Kato, *Perturbation Theory for Linear Operators*, Springer-Verlag Berlin-Heidelberg-New York, (1995).
- [22] H. Kielhöfer, *Bifurcation Theory: An Introduction with Applications to PDEs*, Springer-Verlag, Berlin-Heidelberg-New York, (2004).



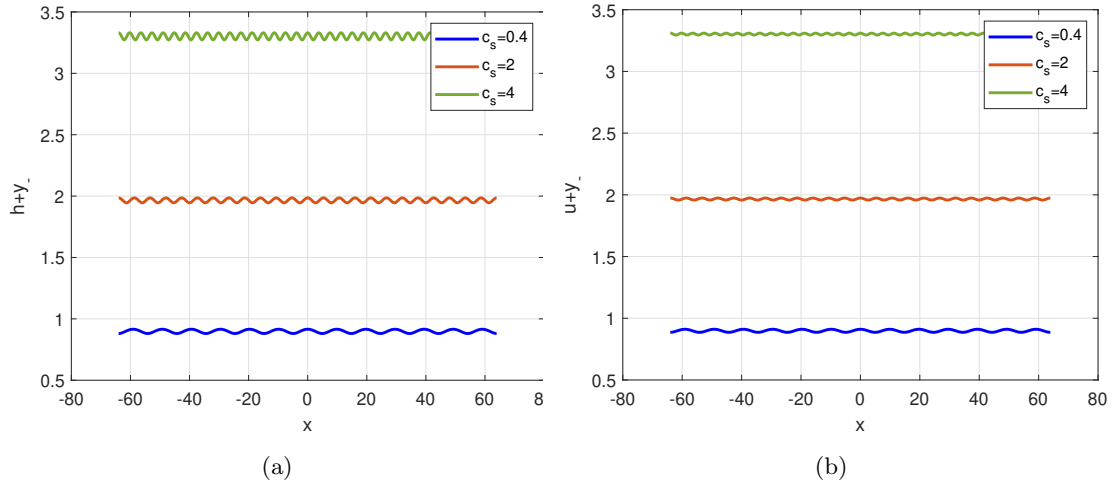


FIGURE 13. Approximations to traveling-wave solutions of (16) for two values of  $c_s$ . Case  $g = g_1(c_s) - 0.001$ . (a)  $\tilde{h} + y_-$  profile; (b)  $\tilde{u} + y_-$  profile.

- [23] T. Kakutani, H. Ono, T. Taniuti, C.-C. Wei, *Reductive perturbation method in nonlinear wave propagation ii. application to hydromagnetic waves in cold plasma*, Journal of the Physical Society of Japan 24 (5) (1968) 1159–1166 (1968).
- [24] J. Lenells, *Traveling wave solutions of the Camassa-Holm and Korteweg-de Vries equations*. J. Nonlinear Math. Phys. 11, pp. 508–520, (2004).
- [25] J. Lenells, *Traveling wave solutions of the Camassa-Holm equation*. J. Differential Equations, 217, pp. 393–430, (2005).
- [26] P. L. Lions, *The concentration-compactness principle in the calculus of variations. The locally compact case. Part I and Part II*. Ann. Inst. Henri Poincaré Sect A (N.S.) 1, pp. 109-145 and pp. 223-283, (1984).
- [27] E. Lombardi, *Oscillatory Integrals and Phenomena Beyond all Algebraic Orders*, Springer-Verlag, Berlin-Heidelberg, (2000).
- [28] X. Pu, M. Li, *Kdv limit of the hydromagnetic waves in cold plasma*, Zeitschrift für angewandte Mathematik und Physik 70 (1) (2019) 32 (2019).
- [29] E. Stein, *Singular Integrals and Differentiability Properties of Functions (PMS-30)* Princeton University Press, (1970)
- [30] J. F. Toland, *Existence of symmetric homo-clinic orbits for systems of Euler-Lagrange equations*, A. M. S. Proceedings of Symposia in Pure Mathematics, 45(2), 447-459, (1986).
- [31] J. Zhou, L. Tian, *Solitons, peakons and periodic cusp wave solutions for the Fornberg-Whitham equation*, Nonlinear Anal., 11, 356-363, (2010).

## APPENDIX A. A PROCEDURE FOR THE NUMERICAL GENERATION OF TRAVELING WAVES

The numerical method to approximate solutions of (32) is here formulated. The equation is first written in fixed-point form

$$\mathcal{L}\tilde{u} = \mathcal{N}(\tilde{u}), \quad (38)$$

(we occasionally recover the tilde in the notation, for reasons that will become evident below) where  $\mathcal{L}$  is a linear operator and  $\mathcal{N}(\tilde{u})$  gathers for the nonlinear terms involving  $\tilde{u}$  and its derivatives up to fourth order. Explicitly

$$\begin{aligned} \mathcal{L} &= \alpha_{\pm} \mathcal{J}^2 + \frac{y_{\pm}}{2} \partial_x^2 - \frac{1}{2} \mathcal{J}, \\ \mathcal{N}(\tilde{u}) &= -\frac{1}{2} \left( \frac{3}{2} \mathcal{J} (\mathcal{J} \tilde{u})^2 + \partial_x (\tilde{u}_x \mathcal{J} \tilde{u}) - \frac{1}{2} \mathcal{J} (\tilde{u}_x^2) \right). \end{aligned}$$

Equation (38) is iteratively solved from an approximation to (32) on a long enough interval with periodic boundary conditions given by a Fourier collocation method. Let  $N \geq 1$  be an even integer and let

$$x_j = -l + j\Delta x, \quad j = 0, \dots, N-1, \Delta x = 2l/N, \quad (39)$$

be a uniform grid of collocation points on  $(-l, l)$ . We consider the finite dimensional space

$$S_N = \text{span}\{e^{ik\pi(x+l)/l}, k \in \mathbb{Z}, -\frac{N}{2} \leq k \leq \frac{N}{2} - 1\},$$

and define the spectral Fourier collocation approximation to a solution  $\tilde{u}$  of the periodic problem associated to (32) on  $(-l, l)$  as  $\tilde{u}^N \in S_N$  satisfying (38) at the collocation points (39). The approximation  $\tilde{u}^N$  is typically represented by the nodal values

$$\tilde{u}_{\Delta} = (\tilde{u}_0, \dots, \tilde{u}_{N-1})^T, \quad (40)$$

with  $\tilde{u}_j = \tilde{u}^N(x_j)$ ,  $j = 0, \dots, N-1$  as approximations to the nodal values of the solution  $\tilde{u}(x_j)$ . Thus the algebraic system satisfied by (40) is of the form

$$\mathcal{L}_{\Delta} \tilde{u}_{\Delta} = \mathcal{N}_{\Delta}(\tilde{u}_{\Delta}), \quad (41)$$

where

$$\begin{aligned} \mathcal{L}_{\Delta} &= \alpha_{\pm} (I_N - D_N^2)^2 + \frac{y_{\pm}}{2} D_N^2 - \frac{1}{2} (I_N - D_N^2), \\ \mathcal{N}_{\Delta}(\tilde{u}_{\Delta}) &= -\frac{1}{2} \left( \frac{3}{2} (I_N - D_N^2) ((I_N - D_N^2) \tilde{u}_{\Delta})^2 + D_N (D_N \tilde{u}_{\Delta} \cdot (I_N - D_N^2) \tilde{u}_{\Delta}) \right. \\ &\quad \left. - \frac{1}{2} (I_N - D_N^2) ((D_N \tilde{u}_{\Delta})^2) \right). \end{aligned}$$

where  $I_N$  denotes the  $N \times N$  identity matrix,  $D_N$  stands for the pseudospectral differentiation matrix, [7], and the dots in the nonlinear part  $\mathcal{N}_{\Delta}(\tilde{u}_{\Delta})$  denotes Hadamard products of the corresponding vectors. The fixed-point system (41) is implemented by writing its Fourier representation (in terms of the discrete Fourier components of the vectors (40) via Discrete Fourier Transform) and solving iteratively the resulting algebraic system. A typical iterative resolution consists of combining the Petviashvili method with a vector extrapolation technique to accelerate the convergence. The details can be seen in e. g. [16] and references therein.

After obtaining approximations  $\tilde{u}_\Delta$  to the profile  $\tilde{u}$  solution of (32), then we compute  $u_\Delta = \tilde{u}_\Delta + y$  to approximate (18) for both  $y = y_\pm$  and, finally, we approximate the  $h$  profile from the discrete version of (14)

$$h_\Delta = (I_N - D_N^2)u_\Delta.$$

*Email address:* dalonsoo@ull.edu.es

DEPARTAMENTO DE ANÁLISIS MATEMÁTICO Y INSTITUTO DE MATEMÁTICAS Y APLICACIONES (IMAUULL), UNIVERSIDAD DE LA LAGUNA C/. ASTROFÍSICO FRANCISCO SÁNCHEZ S/N, 38200 - LA LAGUNA, SPAIN.

*Email address:* angeldm@uva.es

APPLIED MATHEMATICS DEPARTMENT, UNIVERSITY OF VALLADOLID, 47011 VALLADOLID, SPAIN

*Email address:* rafael.granero@unican.es

DEPARTAMENTO DE MATEMÁTICAS, ESTADÍSTICA Y COMPUTACIÓN, UNIVERSIDAD DE CANTABRIA. AVDA. LOS CASTROS S/N, SANTANDER, SPAIN.